

Using Eco-cement made from Municipal Solid Waste Incineration Residues as a Mineral Additive for Concrete

Mohammed Hashem



McGill University

Department of Civil Engineering

Montreal, Quebec, Canada

Date: 07/2021

A thesis submitted to McGill University in partial fulfillment of the requirements of the degree of
Master of Engineering

© Mohammed Hashem, 2021

Abstract

Incineration is a widely used approach for managing municipal solid wastes (MSW). However, while this technique substantially reduces waste volume, it does not present a fully circular solution since it generates sizable amounts of residual by-products, most commonly in the form of bottom ash, boiler ash (or fly ash), and waste-lime. These residues are generally unusable and present handling challenges, especially for boiler ash and waste-lime for their high toxicity and heavy metal content. Common handling practices include costly treatment and dumping in specialized landfill sites. This thesis work attempts to address this problem by synthesizing a new form of cementitious material consisting primarily of incineration residues and coined hereinafter “Eco-cement”. Eco-cement is made up of 94% incineration residues and produced through a controlled heat treatment at a maximum temperature of 1100 °C. The synthesis of Eco-cement and the viability of its use as a supplementary cementitious material (SCM) to Portland cement are explored. Analytical characterizations along with performance appraisals based on compressive strength, ASTM standard testing protocols, and durability tests were carried out to appraise and understand the behavior of Eco-cement in concrete. At 15% binder replacement, Eco-cement seemed to lend a sort of hydraulic accelerator effect, recording a 28% increase in one-day compressive strength and a 15% reduction in setting time. The cause of this phenomenon was likely attributed to the high amount of chlorine-containing minerals in Eco-cement, identified as Chlorellestadite and Wadalite. Furthermore, the blended binder increased the ultimate strength of concrete by 6%, reaching 51 MPa in 90 days. The addition of Eco-cement to concrete did not affect the durability and pore structure of the concrete. Eco-cement may very well be a promising recycling solution to a prevailing problem in the modern world, and a much needed waste-derived supplementary cementing material to the ever-growing construction industry.

Résumé

L'incinération est une approche largement utilisée pour gérer les déchets solides municipaux (DSM). Toutefois, bien que cette technique permet de réduire considérablement le volume des déchets, elle ne constitue pas une solution idéale puisqu'elle génère des quantités non négligeables de sous-produits résiduels, le plus souvent sous la forme de mâchefers, de cendres de chaudière (ou cendres volantes) et de chaux résiduelle. Ces résidus sont généralement inutilisables et posent des problèmes de manipulation, en particulier pour les cendres de chaudière et la chaux résiduelle en raison de leur forte toxicité et de leur teneur en métaux lourds. Les pratiques courantes de manipulation de ces matériaux sont impliquent des traitements coûteux et impliquent des déversements dans des sites d'enfouissement spécialisés. Cette thèse tente de résoudre ce problème en synthétisant une nouvelle forme de matériau cimentaire composé principalement de résidus d'incinération et appelé "Eco-ciment". L'éco-ciment est composé à 94% de résidus d'incinération et est produit par un traitement thermique contrôlé à une température maximale de 1100C. La synthèse de l'éco-ciment et la viabilité de son utilisation comme additif minéral complémentaire au ciment Portland sont explorées. Des caractérisations analytiques ainsi que des évaluations de performance basées sur la résistance à la compression, des protocoles d'essai standard ASTM et des tests de durabilité ont été effectués pour évaluer et comprendre le comportement de l'éco-ciment dans le béton. À un niveau de remplacement de 15 %, l'éco-ciment semble avoir un effet d'accélérateur hydraulique, enregistrant une augmentation de 28 % de la résistance à la compression à un (1) jour et une réduction de 15 % du temps de prise du béton. La cause de ce phénomène a probablement été attribuée à la quantité élevée de minéraux contenant du chlore dans l'Eco-ciment, identifiés comme Chlorellestadite et Wadalite. En outre, le mélange de ciment a augmenté la résistance ultime du béton de 6 %, atteignant 51 MPa en 90 jours. L'ajout d'éco-ciment au béton n'a pas affecté la structure des pores du béton, ni sa durabilité. L'éco-ciment pourrait bien être une solution de recyclage prometteuse à un problème prédominant dans le monde moderne, et un matériau complémentaire dérivé des déchets dont l'industrie de la construction en pleine croissance bénéficierait grandement.

Acknowledgements

Fist of all, I would like to extend my gratitude to my supervisor, Professor Yixin Shao, for his invaluable guidance and support throughout this project. I would also like to thank Dr. Zaid Ghouleh for his co-supervision and Dr. Shipeng Zhang for his mentorship and continued assistance.

I would also like to thank Emerald Energy-from-Waste (EEFW), Brampton (ON), for their sponsorship and providing us with the raw materials used in this work. I would also like to thank Dr. Zhen He and Liu Shaoyan from the University of Wuhan, for their help with the heat of hydration analysis. I would also like to extend my gratitude to Dr. Warda Ashraf for her help in reviewing the thesis and her valuable feedback.

Finally, I would like to thank my friends and family for their continued love and support during this project. I would not be where I am today without them.

Table of Contents

Abstract.....	I
Résumé	II
Acknowledgements.....	III
Table of Contents.....	IV
List of Figures	VI
List of Tables	VII
1 Introduction	1
2 Literature Review	3
2.1 Environmental impacts	3
2.1.1 MSW processing.....	4
2.1.2 Cement production.....	6
2.2 Concrete additives	7
2.3 Alternate cement replacements in the literature.....	12
2.3.1 Alternative additives	12
2.3.2 History of MSWI residues in cement	14
2.4 Objectives.....	15
3 Experimental Program	16
3.1 Materials	16
3.2 Eco-cement blend design.....	17
3.3 Production of Eco-cement	21
3.4 Characterization of Eco-cement	26
3.5 Casting procedures	27
3.6 Testing.....	30
3.6.1 Mineral composition	30
3.6.2 Compressive strength, setting, and hydraulic performance.....	31
3.6.3 Pore structure analysis and durability testing	35
4 Results and Discussion	37
4.1 QXRD	37
4.2 SEM	39
4.3 Compressive strength	40
4.4 Setting time.....	44
4.5 Heat of hydration	45

4.6	SCM classification	49
4.7	Water absorption	51
4.8	Surface resistivity	53
4.9	Freeze/thaw	55
4.10	Leaching	57
5	Conclusions	58
	Future Works	60
	References	61

List of Figures

Figure 1 Incineration process and by-products	5
Figure 2 Eco-cement CAS ternary phase diagram.....	19
Figure 3 Raw MSWI residues	22
Figure 4 Eco-cement disks for clinkering	23
Figure 5 Rotating drum granulator	24
Figure 6 Nodules after clinkering.....	24
Figure 7 Lindberg Blue furnace	25
Figure 8 Eco-cement synthesis process	26
Figure 9 Eco-cement replacement % 28d strength comparison.....	28
Figure 10 Mold for compact making.....	29
Figure 11 Typical concrete and paste samples	30
Figure 12 MTS Sintech 30/G - Compact testing.....	32
Figure 13 MTS Series 315 - Concrete testing.....	33
Figure 14 Vicat needle apparatus	34
Figure 15 Resistivity meter and calibration board.....	35
Figure 16 Thawing (top) and freezing (bottom) set up.....	37
Figure 17 QXRD diffraction pattern for Eco-cement.....	38
Figure 19 SEM of raw Eco-cement	39
Figure 20 EDS of raw Eco-cement	40
Figure 20 Paste compacts compressive strength	41
Figure 21 Concrete compressive strength	43
Figure 22 Vicat needle setting rate.....	44
Figure 23 Vicat needle initial and final time of setting.....	45
Figure 24 Heat of Hydration results	46
Figure 25 Induction (1) and dormant (2) stages	48
Figure 26 Cracking in 50%ECO paste samples	49
Figure 27 Water absorption results for concrete specimens	52
Figure 28 Concrete volume of voids	53
Figure 30 Surface resistivity results	54
Figure 31 Typical concrete cube at 60 freeze/thaw cycles	56
Figure 32 Concrete freeze/thaw results	56

List of Tables

Table 1: Properties of GGBFS from different regions (source: (Juenger, et al., 2012))	11
Table 2 Chemical composition of MSWI residues.....	17
Table 3 Eco-cement blend proportions	18
Table 4 Eco-cement blend CAS composition	18
Table 5 Eco-cement oxide and strength correlation.....	20
Table 6 Ratios governing Eco-cement blend design	21
Table 7 Chemical composition of binders.....	27
Table 8 Concrete and paste mix proportions.....	28
Table 9 QXRD of Eco-cement and OPC	37
Table 10 Pozzolanic activity results	50
Table 11 Strength Index of cementitious test.....	50
Table 12 Heavy metal leaching performance	57

1 Introduction

With the ever-increasing growth in population, there is no doubt that municipal solid waste (MSW) production is on the rise. The World Bank estimated global MSW production to be 1.3 billion tons (Bt) in 2012 and expected to reach 2.2 Bt by 2025 (Hoornweg & Bhada-Tata, 2012). This presents an even greater concern in densely populated cities and countries; for instance, China recorded a 45.2% increase in MSW production between 2009 and 2018 (Kosajan, et al., 2020), while Sharholy, et al. state that major cities in India observed increases of the order of 800% since 1947 (Sharholy, et al., 2008). With continued industrialization, it is no surprise that MSW generation has sky-rocketed, especially when considering the broad range of wastes that are categorized as MSW. MSW consists of food waste, paper, wood, glass, and other refuse materials consumed by everyday residential and commercial activities (Wang, et al., 2018). MSW management is a difficult process that has many intricacies; it involves collection, transfer, and treatment of the waste. Treating MSW is vital to maintain the health of the population, increase environmental quality, and ensure sustainability. Many different MSW management methods have been adopted throughout the years by municipalities, ranging from common strategies such as landfilling and incineration to more advanced recycling techniques and biological treatments in more recent times.

Incineration is a widely used approach to manage solid waste. It allows for weight and volume reduction as well as energy recovery (Shen, et al., 2018). However, there are multiple by-products that are co-generated by this approach which include bottom ash, boiler ash, air pollution control (APC) lime (or waste-lime), and carbon dioxide. It is challenging and costly to manage the unstable ash residues of incineration; boiler ash (also referred to as fly ash in varying incinerator

installations) in particular poses a significant threat due to its fineness and high heavy metal content (Wang, et al., 2019). Of the many stabilization and fixation techniques discussed in the literature, a promising approach presented by a group of researchers at McGill University offers the unique conversion of incineration residues into a cement-like material, Eco-cement, activated by carbonation for binding strength (Ghouleh & Shao, 2018; Ghouleh, et al., 2021). Eco-cement consisted of up to 94% incineration residues and was synthesized at a temperature of 1100 °C. The high temperature processing effectively destroys the organic contaminants of dioxins, furans, VOCs, and PAHs commonly found in the ash residues. Moreover, the final phases that form in Eco-cement have been shown to molecularly entrap and stabilize the heavy metals. Incineration residues can therefore be suitably valorized to serve as a cementing material.

Eco-cement has successfully been demonstrated as a stand-alone binder in concrete, provided that it is activated for binding strength via carbonation (i.e. reacting with carbon dioxide). While carbonation-curing has been gaining increased traction in recent years as a more sustainable concrete manufacturing approach, it has not been commercially implemented to any significant degree yet. This may take years. Another possible and market-ready use of Eco-cement could be as a partial replacement of ordinary Portland cement (OPC). Partial replacement of cement with supplementary cementitious materials (SCM) is a very common practice due to the countless advantages provided by commercial additives. Fly ash from coal burning plants and GGBFS (Ground Granulated Blast Furnace Slag) from iron making processes are among the most common types of SCMs. These SCMs can provide higher compressive strength, lower porosity, and increased durability in concrete. This thesis aims to evaluate the viability of using Eco-cement as an SCM in concrete by adopting a systematic performance-based approach consisting of

standardized tests and comparison to commonly used commercial SCMs. In addition to compressive strength, Eco-cement use was further evaluated by measuring fresh concrete properties and carrying out durability tests appraising its resistance to frost damage. Analytical techniques used included X-ray Fluorescence (XRF), Quantitative X-ray Diffraction (QXRD), Scanning Electron Microscopy (SEM), and Heat of hydration calorimetry.

The first objective of this work was to successfully synthesize Eco-cement with compositional and mineralogical traits that promote cementitious behaviour. Next, was to evaluate Eco-cement as a supplementing mineral additive in traditional Portland concrete and compare it to commercial coal-fly ash and GGBFS.

2 Literature Review

This chapter introduces MSW and its impact on the world, along with the advantages and disadvantages of MSW incineration. The chapter also discusses the environmental impact of cement production on a global scale, highlighting the advantage of replacing traditional cement with more environmentally conscious products. The second portion of this literature review introduces and discusses commonly used SCMs, which will be used to evaluate Eco-cement. Finally, different innovative and unconventional SCMs developed from the by-products of other industries are presented along with other versions of MSW incineration residue-based additives.

2.1 Environmental impacts

MSW management is not a very well optimized process. Landfills are still commonly used despite efforts made to transition into more environmentally conscious practices such as recycling. Furthermore, cement production is a process that is far from ideal from an

environmental point of view due to its high energy demand and greenhouse gas emissions. In this section, the environmental merits of reusing MSWI residue as a cement replacement are discussed.

2.1.1.1 MSW processing

Although developed countries, especially those with high population densities, have moved away from using landfills, it is still the predominant method of handling MSW in emerging countries. In 2016, 60% of the total MSW of China was dumped in landfills (Yao, et al., 2019). Other than the obvious suboptimal land use, unpleasant odours, and a general decrease in the quality of life near landfill sites, landfills have much more serious effects, such as methane release and contamination of soil and underground water reserves. Water contaminated by landfill leachates poses a threat to local resource users and surrounding nature (Mor, et al., 2006). More sustainable approaches are being considered to decrease the occupancy of landfills. In Europe, for example, 15% of the total amount of municipal waste is being redirected from landfills to other treatment options such as recycling. This leads to a decreased impact on the environment, cost, and energy (Eriksson, et al., 2005).

Another rather common solution to this MSW epidemic is incineration. Many countries with limited space availability such as Denmark, Germany, and Sweden have been using incineration as their preferred method of MSW mitigation (Reike, et al., 2018). The two main advantages of incineration are 90% waste volume reduction and cost efficiency due to the generation of energy from combustion (Santos, et al., 2013). When waste is burnt in an incinerator, the heavier combustion by-products fall to the bottom of the combustion chamber in the form of bottom ash, while the lighter particulate ash material gets drawn by the upward

moving flue gas. This hot flue gas passes through the heat recovery boilers to generate high-pressure steam, which in turn runs a mechanical turbine to produce electricity. Depending on the incinerator setup, boiler ash is separated from the flue-gas either by an Electrostatic Precipitator (ESP) or filtered using a baghouse assembly. Downstream air pollution control (APC) systems use lime to neutralize the acidity of the flue gas and control NO_x/SO_x emissions. Once lime is fully expended, it is collected separately as another waste ash stream, also known as APC lime. The treated and filtered flue-gas is then safely released through the smokestack. An illustration of the collection locations of MSWI residues within an incinerator is shown in Figure 1.

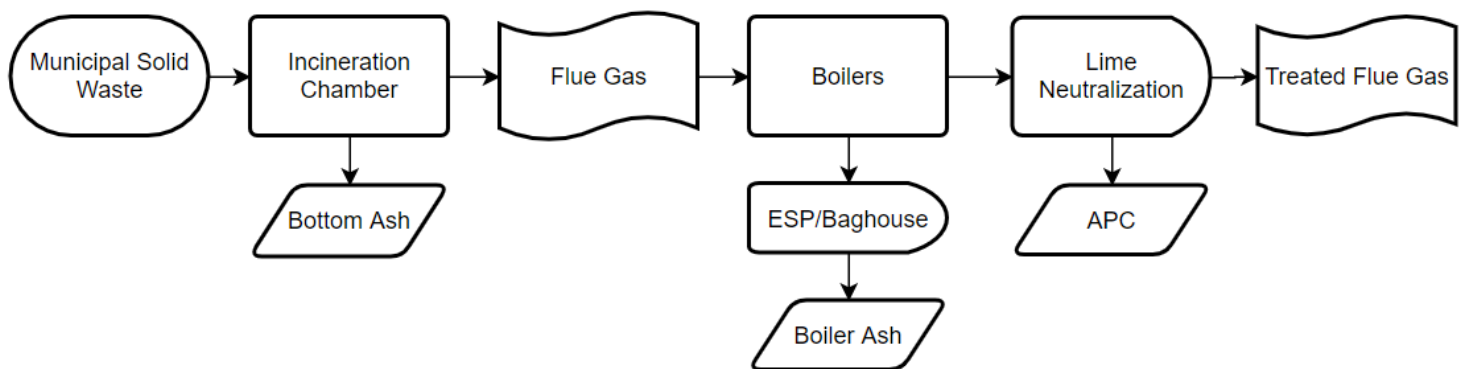


Figure 1 Incineration process and by-products

At a glance, incineration would seem to have solved many of the problems facing MSW management; however, one must consider the residue by-products, their associated danger to the environment, and treatment options. Two of these residues - boiler ash and APC - are particularly hazardous due to their high content of heavy metals, and their large amounts of soluble salts (Quina, et al., 2014). While it is possible to treat these toxic by-products and then dump them into specialized landfills, this operation is very costly. Therefore, it is highly

recommended to treat and recycle them as raw materials in other manufacturing processes as much as possible (Quina, et al.,2007).

These residues are also very high in silica, calcium, and alumina, which happen to be the base oxides used in cement production (Tang, et al., 2018). This makes a strong argument in favour of recycling these ashes into a cementing material. Developing a final concrete mix with waste-derived cementitious materials has a twofold environmental impact. Firstly, it reduces the amount of cement clinker needed in concrete, thereby reducing the product's embodied energy and carbon footprints. Additionally, the recycling of MSW incineration residues as a raw clinker feed solves a major health and safety predicament by molecularly entrapping and stabilizing the toxic heavy metals present in these residue ashes. Multiple works in the literature have highlighted the effectiveness of using incineration residues in cementitious materials (Ashraf, et al., 2019; Ghoulah & Shao, 2018; Zhang, et al., 2020). In this work, Eco-cement uses up to 94% of its raw materials from incineration residues.

2.1.2 Cement production

The amount of cement produced worldwide has increased from around 2 billion tons in 2005 to 2.8 billion tonnes in 2010 (Ezema, 2019), and is expected to reach 4 billion tonnes per year by 2050 (Schneider, et al., 2011). The production of Portland cement is a multistep process. The main steps are briefly described as follows. Raw materials high in calcium carbonate (limestone), silica, and alumina (clay) are finely ground together. This mixture is calcined and then processed in a kiln at a temperature of 1450 °C and the final melt is quickly quenched to produce what is known as clinker. The clinker is then ground with gypsum to produce the abundantly used final Portland cement product (Habert, 2014). The clinkering and calcination steps produce large

amounts of CO₂; manufacturing 1 tonne of cement releases up to 0.97 tonnes of CO₂, making the cement production industry the third largest emitter of CO₂ (Dhawan, et al., 2020). The environmental impact of cement production does not stop at energy consumption and CO₂ generation. It also consumes immense amounts of virgin materials reaching up to 1.5 tonnes of raw resources used per tonne of cement produced (Rashad, 2018). One solution is to use by-products of other manufacturing processes as partial replacements in concrete. This will allow for the reduction in the amount of virgin material used, as well as a cutback in the energy needed and CO₂ generated from the reduction of clinker.

2.2 Concrete additives

SCMs are additives to cement that can provide a wide array of advantages from better workability to improvements in compressive strength and durability. Air-entraining, water-reducing, retarding, accelerating, and plasticizer admixtures are among the most common types of SCMs. The incorporation of SCMs is a common approach to improving concrete longevity and overall service performance. It has been shown that the incorporation of admixtures such as limestone, natural pozzolans, blast furnace slag, and/or silica fume improves the mechanical properties of mortars and concrete mixes (Makhloufi, et al., 2014). Furthermore, the use of these additives, where no additional clinkering is needed, significantly reduces the energy consumed as well as the CO₂ emitted per ton of cement. For example, blast furnace slag, which must be processed and ground before being used as an SCM, still requires only about 10% of the energy needed to produce an equivalent amount of pure cement (Shia & Qianb, 2000). SCMs are often the by-products of other industrial processes such as blast furnace slag from pig iron production and fly ash from coal-burning power plants. Adding such materials to a cement mixture not only

enhances the physical properties of the resulting concrete, but also greatly reduces the environmental impact. This is achieved through the reutilization of industry by-products as well as a decrease in CO₂ emissions (Lothenbach, et al., 2011).

The demand for high quality SCMs shows the importance of these mineral admixtures in the field of concrete manufacturing; the world average clinker factor (percentage of clinker in cement) decreased from 0.85 in 2003 to 0.77 in 2010, and this number is expected to decrease down to 0.71 in the coming years. Holcim - one of the largest building materials and aggregate companies in the world - stated that blended cements represented 75% of their cement production in 2009, compared to 39% in 1995 (Juenger, et al., 2012). The amount of SCMs added to the cementing mix must be specified and moderated by different governing entities. In Canada, the requirements for concrete made with and without SCMs are covered by CSA A23.1. CSA specifications dealing with blended hydraulic cements stipulate a maximum content of 70, 40 and 10% of GGBFS, fly ash, and silica fume, respectively. The percentage is expressed by the total weight of cementitious materials (Bouzoubaâ & Fournier, 2003).

One of the most popular SCMs used in concrete design are classified as pozzolans. Pozzolans have a very high content of reactive silica (or alumina). By themselves, pozzolans have little to no cementitious properties; however, in the presence of moisture, they will chemically react with alkalis to form cementing reaction products (Setina, et al., 2013). The blending of SCMs with Portland cement leads to a more complicated system where the hydration of the cement and the hydraulic reactions of SCMs occur simultaneously or sequentially. Pozzolans generally react with cement's generated hydrous alkali phases, especially calcium hydroxide, to form additional calcium silicate hydrate (C-S-H), the most important reaction product of cement and

one responsible for concrete's binding strength (Korpa, et al., 2008; Lothenbach, et al., 2011). The advantages of pozzolanic additives are numerous and include lower strain due to creep, lower long-term drying shrinkage, higher ultimate strength, lower permeability, inhibition of alkali silica reaction, and improved resistance to sulfuric acid and hydrochloric acid (Khatri, et al., 1995; Massazza, 1993; Toan, et al., 2020).

Fly ash, a by-product of coal burning, is a very commonly used pozzolan in cement mixtures. ASTM broadly classifies fly ash into two categories, class F and class C. This separation represents differences in composition and pozzolanic properties. Class F fly ash is usually produced by burning anthracite or bituminous coal and is purely pozzolanic, while class C fly ash is normally produced by burning sub-bituminous coal or lignite and exhibits some self cementing properties (Shetty, 2005). The main active portion of fly ash consists of silica and alumina. Part of the Al_2O_3 exists as mullite ($3\text{Al}_2\text{O}_3 \cdot 2\text{SiO}_2$), and the remainder is contained in an amorphous glass phase. Other crystalline constituents found to a lesser degree are magnetite (Fe_3O_4) and hematite (Fe_2O_3), and rarely some merwinite [$\text{Ca}_3\text{Mg}(\text{SiO}_4)_2$] and melilite. The reaction products resulting from the pozzolanic reaction are mainly amorphous C-S-(A)-H, C_4AH_{13} , and C_2ASH_8 (Juenger, et al., 2012). Although research shows that any replacement of cement with fly ash between 15% and 35% by weight will not have a negative impact on compressive and flexural strength of concrete, manufacturers usually limit the amount of fly ash used to 25%, with the typical replacement level being around 15%. Other research shows that high volume replacement of cement with 50-60% fly ash (High Volume Fly Ash Concrete) also resulted in concrete with high strength and durability (Dhawana, et al., 2020).

Fly ash has been shown to enhance the hardened properties as well as the fresh properties of concrete in the long run, compensating for the sacrifice in early age strength. Fly ash experiences a slow pozzolanic reaction; class F fly ash shows strength improvement after nearly 4 weeks. Fly ash also improves the workability of fresh concrete by coating and lubricating the aggregate particles. The spherical shape of the fly ash particles reduces the friction at the aggregate paste interface, producing a ball bearing effect at the point of aggregate contact. Furthermore, bleeding in fly ash concrete is significantly reduced, and other properties like cohesiveness, pumping characteristics, and surface finish are improved (Marthong & Agrawal, 2012). As the world moves towards cleaner energy production, it is inevitable that coal burning will be reduced dramatically, and hence fly ash supply. Suitable substitutes need to be explored. Eco-cement could be one such solution.

Another common type of SCMs added to concrete for their contribution to ultimate strength are classified as cementitious or hydraulic materials. Unlike pozzolans, these SCMs react directly with water to produce cementitious compounds. GGBFS is a popular choice of latent hydraulic SCMs in the concrete industry. It is a by-product from the production of iron and must be periodically removed from the blast furnace (Neuwald, 2010). It forms by fusion of the gangue material of the iron ore, mainly silica and alumina compounds, with calcium and magnesium oxides of the thermally decomposed carbonatic flux and combustion residues of the coke. These reactions take place at temperatures between 1300 and 1600°C (Juenger, et al., 2012). The input material controls the chemical properties of the slag, while the cooling manner determines the physical and mineralogical properties. To form a hydraulic cementitious material, the slag must be rapidly cooled in order to produce a reactive amorphous glass phase that is ideal for use in

concrete construction (Neuwald, 2010). This high glass content is the prerequisite for the latent hydraulic reactivity of GGBFS, which, when ground, makes a highly effective SCM (Hooton, 1987). The contents of the slag differ depending on the input material, which vary from plant to plant and region to region. Table 1 shows the different oxide percentages of slags collected from different regional sources. However, in general the reactivity of a slag is directly proportional to its contents of CaO, MgO, Na₂O, and Al₂O₃, and inversely proportional to its contents of SiO₂, FeO, TiO₂, MnO, and MnS. A high CaO/SiO₂ ratio generally indicates good reactivity (Juenger, et al., 2012).

Table 1: Properties of GGBFS from different regions (source: (Juenger, et al., 2012))

Component (%)	North America	Central and Latin America	Western Europe	Eastern Europe	India, Japan, Australia
SiO ₂	34.6-39.9	33.5-34.8	32.0-39.4	33.5-41.5	32.6-36.9
CaO	35.3-42.8	39.1-43.8	34.9-44.3	36.9-47.5	33.0-43.0
Al ₂ O ₃	6.6-11.5	10.0-13.0	9.5-12.5	5.5-12.4	10.2-19.3
MgO	7.0-13.1	5.9-9.9	5.0-13.4	2.5-11.2	4.9-13.8
TiO ₂	0.3-0.8	0.5-0.6	0.4-1.3	0.2-1.3	0.6-2.1
Na ₂ O	0.3-0.8	0.4-0.8	0.3-1.2	0.6-1.1	0.4-0.8
SO ₃	2.0-3.0	1.1-3.7	2.0-4.5	1.6-3.8	1.7-4.0
CaO/SiO ₂	0.9-1.2	1.1-1.3	1.0-1.3	0.9-1.3	0.9-1.3

Upon hydration, GGBFS produces very similar hydration products to Portland cement, i.e., C-S-H and ettringite (Regourd, et al., 1983). Despite its hydraulic behaviour, GGBFS reacts very slowly with water alone. However, when mixed with OPC, the calcium hydroxide and gypsum from the OPC act as activators (Richardson, et al., 1989). In this mixture, the main phases observed in the hydrated product are C-S-H, calcium hydroxide, and sulpho-aluminate hydrates (Richardson & Groves, 1992).

In normal cement, the most common percentage of cement replacement with GGBFS is around 30% by weight, although other applications can reach up to 85% (Rashad, 2018). It has been shown that the inclusion of GGBFS as an SCM resulted in a final concrete paste with better pore size distribution and a denser ITZ. These properties associate improvements in concrete durability and reduced susceptibility to damage incurred by aggressive contaminants that normally affect concrete during its service-life. Furthermore, GGBFS blended cements have been demonstrated to achieve higher performing concrete strengths (Duan P, et al., 2013).

2.3 Alternate cement replacements in the literature

In this chapter, efforts of using innovative materials and industry by-products as SCMs will be reviewed to determine common testing procedures and outline any interesting findings. Furthermore, previous works using MSW incineration residues as a cement replacement will be reviewed.

2.3.1 Alternative additives

The literature contains numerous examples of using unconventional materials as cement replacements and SCMs. El-Dieb & Kanaan (2018) studied the use of ceramic waste powder (CWP) as a partial cement replacement. Evaluation based on fresh concrete properties, compressive strength, and durability were performed. It was found that CWP produced a better performing concrete mix with a significant decrease of permeable pores leading to a more durable final product (El-Dieb & Kanaan, 2018). Another 2018 study by Ghorbani et al. used marble and granite dust (MGD) as a partial cement replacement. The study showed that the use of MGD did not significantly affect the compressive strength of concrete. The study's main

contribution was linking MGD replacement to protection of steel rebar, which remained uncorroded despite being exposed to NaCl for 92 days (Ghorbani, et al., 2018). Another study done by Ghorbani explored the use of granite waste dust (GWD) as a partial cement replacement. The main focus of the study was the effect of harsh exposure conditions on the concrete. The concrete was exposed to 5% by weight of NaCl and H₂SO₄ solutions for 90 days. The results showed that using GWD at 20% replacement led to significantly better resistance to the acid and chloride attacks, without affecting the mechanical properties of the concrete (Ghorbani, et al., 2019). A study by Mashaly et al. linked 20% replacement of cement with granite sludge (from ornamental stone manufacturing) to increased resistance to sulfate attack and freeze/thaw, with no sacrifice in strength (Mashaly, et al., 2018). The use of rice husk ash as a partial cement replacement was demonstrated by Zareei et al. At 15% loading rate, this rice mill by-product was found to increase compressive strength by 20% and decrease water absorption and chloride penetration (Zareei, et al., 2017). Palm oil clinker powder, a byproduct of the palm oil industry, was used as a partial cement replacement in mortars by Nayaka et al. The use of this powder recorded slight increases in mechanical properties and a 32% reduction in total carbon footprint. The final recommendation for optimal results was 40% replacement (Nayaka, et al., 2018).

Analyzing the mentioned studies, as well as many more available in the literature, shows that cement replacement by other industry by-products is a viable technique that reduces the carbon footprint and almost always improves concrete durability with little to no sacrifice in compressive strength.

2.3.2 History of MSWI residues in cement

Many works have been documented in the literature on the use of MSW incineration residues in the cement industry. One of the first trials was performed in 1999 by Shimoda and Yokoyama where a powder mixture consisting of 50% MSWI residues was processed similarly to OPC in a cement kiln at 1350 °C. The results were also similar to OPC, producing a concrete with a 28-day hydration compressive strength of 53 MPa (Shimoda & Yokoyama, 1999). Similarly, Kikuchi utilized a mixture of 40% MSWI and 50% limestone. The results showed a mortar compressive strength of up to 35 MPa in 28 days of hydration (Kikuchi, 2001). In more recent years, more studies have explored the use of MSWI as a component in cement production; for example, in 2008, Singh et al. used a mix containing boiler ash and bottom ash from MSWI (Singh, et al., 2008); in 2011, Wu et al. created a mix with 30% MSWI products to produce sulfoaluminate cement (Wu, et al., 2011); in 2014, Guo et al. produced a calcium sulfoaluminate cement with 30% boiler ash from MSWI (Guo, et al., 2014), to mention a few.

Waste derived cementing materials similar to the one explored in this work, was first published in 2018 by Ghoulé and Shao. MSWI residues collected in Quebec, Canada, were used with the addition of 15% hydrated lime and silica and clinkered at 1000°C, similar to the operating temperatures of a typical incinerator. The generated cement exhibited excellent binding capability when carbonated rather than being traditionally hydration cured. This was ideal since CO₂ is produced in abundance during incineration. Within only 2 hours of carbonation, the paste specimens recorded a compressive strength of 53 MPa, comparable to that of control OPC paste at 63 MPa (Ghoulé & Shao, 2018). This idea of transforming incineration plants into a cleaner

cement production facility was further expanded upon by Ashraf et al. in 2019. This time, up to 94% of the Eco-cement was MSWI waste with only 6% additional virgin material and clinkering at 1100°C. Paste compacts were made out of the material and were carbonated for 2 hours which led to an average compressive strength of 55 MPa (Ashraf, et al., 2019).

In 2020, Zhang et al. also produced a cementing material made out of 94% MSWI residues. This mix was clinkered at 1100°C and contained very few additional raw materials. The reactive minerals in the mixture were found to be belite and chlorellestadite. On its own, the material performed similarly to OPC when hydrated, but upon carbonation, it substantially outperformed OPC (Zhang, et al., 2020). Zhang et al. then focused their study on creating the optimal Eco-admixture blend with a focus on dry cast carbonation curing.

The synthetic cementitious material targeted by this thesis similarly recycled 94% MSWI residues. Unlike Zhang et al., however, the Eco-cement product was not explored as a binder activated by carbonation curing, but rather as an SCM in traditional hydration-cured wet-cast concrete. The common industry practice uses 15% replacement levels, which will be emulated in this study.

2.4 Objectives

The objectives of this study can be split into two main sections:

1. To successfully synthesis a consistent Eco-cement product that performs well in benchmark validation tests. This is done by varying multiple parameters such as stoichiometric residue mixes and clinkering conditions.

2. To evaluate Eco-cement's viability as a concrete additive. This is done through assessing performance versus traditional SCMs according to standardized ASTM tests. Evaluation is done mainly based on strength performance, hydration properties, and durability testing.

3 Experimental Program

This chapter will outline the materials used in this work. The process of Eco-cement synthesis is presented in detail. Evaluation methods and tests will also be introduced.

3.1 Materials

Bottom ash, boiler ash, and APC lime were collected from Emerald EFW Incinerator located in Ontario, Canada. For reference batches, CAN/CSA-A3001 (Canadian Standards Association) Type GU ordinary Portland cement (Cement Quebec) was used for this work. The additives used as a reference in this work were NewCem (Lafarge NewCem[®]), which is a commercially available GGBFS, and coal-sourced type CI fly ash. Coarse and fine granite with 1.6% and 4.3% absorptions, respectively, were used as aggregates in concrete samples.

A Panalytic PW2240 spectrometer was used to perform X-Ray Fluorescence (XRF) analysis on small amounts of the residues. The quartering method in ASTM C702 was used to obtain appropriate amounts of the residues that are representative of the entire batch. The chemical compositions of the MSWI residues are shown in Table 2. The high content of CaO, SiO₂, and Al₂O₃ make these residues prime candidates for use as raw feed for cement. APC can act as the primary source of CaO, while the combination of bottom ash and boiler ash supply the necessary SiO₂ and Al₂O₃ contents. The loss on ignition (LOI) content for each residue was determined based on ASTM D7348. Bottom ash and APC have significantly higher LOI values, indicating a higher

amount of combustible (organic) components. Finally, the total chlorine content was determined using instrumental neutron activation analysis (INAA). APC in particular contained a high amount of Cl.

Table 2 Chemical composition of MSWI residues

Oxide	Composition (% wt)		
	Bottom ash	Boiler ash	APC
SiO ₂	26.74	26.94	2.46
Al ₂ O ₃	9.54	15.21	1.45
Fe ₂ O ₃	6.23	4.64	0.39
MnO	0.13	0.33	0.03
MgO	2.25	4.11	1.3
CaO	16.13	39.93	49.15
Na ₂ O	2.39	—	—
K ₂ O	1.09	0.07	0.64
TiO ₂	1.91	4.79	0.25
P ₂ O ₅	1.84	3.38	0.09
LOI	29.61	0.11	29.49
Cl	2.08	0.22	14.78

3.2 Eco-cement blend design

Multiple blends were prepared using different proportions of MSWI residues. The blends were ranked based on their hydrated compressive strength at 7 and 28 days. The performance of each blend is shown in Table 3. Based on these criteria, blend G was chosen in this study for further investigation as it demonstrated the most promising cementitious behavior.

Table 3 Eco-cement blend proportions

Blend	MSWI residues (%)			Additives (%)		Hydraulic compact strength (MPa)	
	APC	Boiler ash	Bottom ash	CaO	SiO ₂	7d	28d
A	50	15	35	-	-	2.1	4.9
B	50	20	30	-	-	3.7	7.3
C	42.9	19.1	33.3	4.7	-	7.5	16.1
D	45	30	25	-	-	5.0	11.6
E	45	25	30	-	-	5.4	13.6
F	36.8	29.4	29.4	2.95	1.45	8.8	21.4
G	36.03	28.8	28.8	4.9	1.47	11.2	28.9

The clinkering temperature for Eco-cement was fixed at 1100 °C. This relatively low temperature restricts the formation of high energy cementitious phases such as C₃S. Instead, low energy phases such as C₂S (Belite) tend to form. Belite has four polymorphs that exhibit hydraulic behaviour α , α'_H , α'_L and β_H -C₂S (Mazouzi, et al., 2014). Given that Belite was the most likely phase to form during clinkering, multiple blends were designed to target this region in the CAS ternary system. The C₂S region on the CAS phase diagram was derived from Masakatsu Hasegawa's work on the thermodynamics of phase diagrams (Hasegawa, 2014). The normalized % weight of each oxide in the blends was calculated (Table 4) and plotted on a CAS ternary phase diagram as shown in Figure 2.

Table 4 Eco-cement blend CAS composition

Oxide	Composition (% wt)								Boiler ash	Bottom ash	APC
	A	B	C	D	E	F	G	OPC			
SiO ₂	25.58	24.95	24.93	25.77	26.39	28.58	27.74	22.76	32.82	51.02	4.64
Al ₂ O ₃	11.10	11.30	11.06	12.34	12.17	12.31	11.91	5.07	18.53	18.20	2.73
CaO	63.32	63.75	64.01	61.89	61.44	59.12	60.35	72.17	48.65	30.78	92.63

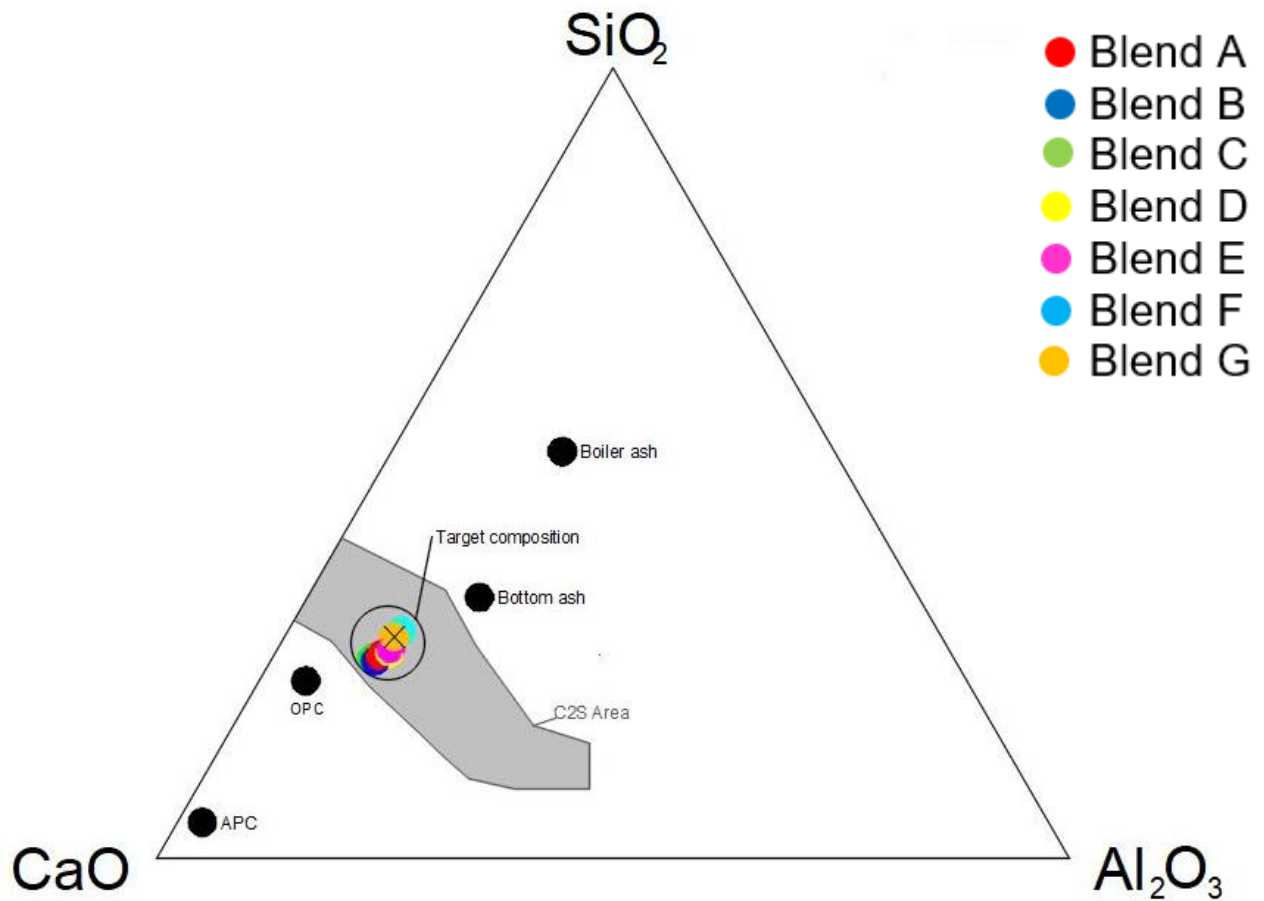


Figure 2 Eco-cement CAS ternary phase diagram

The blend designs were purposefully chosen to increase the reactivity of the C_2S polymorphs in Eco-cement. The reactivity depends on multiple factors including other stabilizing oxides present in the system. Reactivity was optimized by altering the available alkaline oxides such as Na_2O , K_2O , MnO , P_2O_5 and Fe_2O_3 which help stabilize the α and β polymorphs of belite (Ghosh, et al., 1979; Gies & Knöfel, 1986). In Eco-cement, the oxides with the most obvious correlation with strength were MnO , TiO_2 and P_2O_5 (Table 5).

Table 5 Eco-cement oxide and strength correlation

Oxide	Composition (% wt)						
	A	B	C	D	E	F	G
SiO ₂	21.94	21.46	21.48	22.06	22.53	24.44	23.84
Al ₂ O ₃	9.52	9.71	9.53	10.56	10.39	10.52	10.24
Fe ₂ O ₃	4.61	4.38	4.45	4.34	4.55	4.50	4.38
MnO	0.16	0.18	0.17	0.20	0.19	0.20	0.19
MgO	3.08	3.15	2.97	3.31	3.25	3.16	3.08
CaO	54.31	54.81	55.14	52.98	52.46	50.56	51.85
Na ₂ O	1.25	1.05	1.13	0.83	1.02	0.95	0.92
K ₂ O	1.07	0.97	0.93	0.81	0.90	0.78	0.76
TiO₂	2.27	2.43	2.36	2.82	2.67	2.78	2.70
P₂O₅	1.79	1.87	1.84	2.10	2.04	2.11	2.05
Compressive Strength (Mpa)	4.9	7.3	16.1	11.6	13.6	21.4	28.9

Interestingly, TiO₂ was found to have a seemingly definite correlation with C₂S hydration and compressive strength. TiO₂ is known to incorporate into cement hydration phases, with a preferential incorporation in C₂S rather than C₃S (Shang, et al., 2017). Furthermore, TiO₂ has been found to promote the formation of C₂S and stabilize it (Liu, et al., 2013). The hydration of C₂S and C₃S are both increased in the presence of TiO₂. This is likely due to the distortion of the crystal matrices from the substitution of the Si⁴⁺ ions by the Ti⁴⁺ ions (Katyal, et al., 1999). An improvement in the compressive strength of concrete in the presence of TiO₂ has also been well documented in the literature, with most studies attributing the increase in strength to the increased formation of belite and alite (Ali & Shadi, 2010; Jalal, et al., 2013; Mohseni, et al., 2016; Praveenkumar, et al., 2019). The addition of TiO₂ nanoparticles in Belite cement increases the total hydration of C₂S by roughly 50% and it causes an acceleration effect on the early age strength of the concrete. This is likely achieved due to the formation of additional nucleation sites

(Lee & Kurtis, 2012). This relationship between TiO_2 and compressive strength was immediately visible in Eco-cement blends.

To add, the Silica Ratio (SR) and Alumina Ratio (AR) were also used as guidance when proportioning the blends. The ratios are calculated as:

$$SR = \frac{\% SiO_2}{\% Al_2O_3 + \% Fe_2O_3}, AR = \frac{\% Al_2O_3}{\% Fe_2O_3}$$

These ratios are a measure of the quality of the residue blends, with typical OPC values of $SR = 1.9-3.2$ and $AR = 1.7-2.5$ (Lin & Lin, 2012). Eco-cement blends with higher SR and AR values consistently reported higher strength results.

All of the aforementioned factors were considered when deciding the proportion of MSWI residues used in each blend. The correlation between TiO_2 , SR, AR, and compressive strength are shown in Table 6.

Table 6 Ratios governing Eco-cement blend design

Parameter	A	B	C	D	E	F	G
TiO_2	2.27	2.43	2.36	2.82	2.67	2.78	2.70
SR	1.55	1.52	1.54	1.48	1.51	1.63	1.63
AR	2.07	2.22	2.14	2.43	2.28	2.34	2.34
Compressive strength (MPa)	4.9	7.3	16.1	11.6	13.6	21.4	28.9

3.3 Production of Eco-cement

The MSWI residues collected from the incinerator had different as-received forms (Figure 3). Bottom ash was collected wet and had to be oven dried at $105^\circ C$ for 24 hours. It was then passed through a 10mm sieve to remove large chunks and other foreign constituents that were

not representative of the material. Boiler ash was also dried at 105°C for 24 hours before processing to remove any moisture. The bottom ash and boiler ash were both pulverized for 2 minutes, using a ring-and-puck vibratory pulveriser, to a consistent size to allow for better powder mixing.



Figure 3 Raw MSWI residues

For each blend, bottom ash, boiler ash, APC lime, and any additives were mixed in a 'V' shaped powder blender for 3 hours. After mixing, the powder had to be formed into green bodies to facilitate handling and promote the melting solid-state sintering during high-temperature clinkering. At first, the powders were mixed with water to produce a paste that could be pressed into disks as shown in Figure 4. This process proved to be very time consuming, taking upwards of 15 minutes to make a single disk.



Figure 4 Eco-cement disks for clinkering

In an attempt to further optimize the process, nodules were made instead of disks. The nodules were prepared in a rotating drum granulator. Multiple factors had to be optimized in order to produce consistent nodules. The first factor was rpm: ranges of 15-40 rpm were tested. Another factor that affected the nodule size was the rotating drum angle, ranging from 10-45°. Finally, and most importantly, the rate and amount of added water to the drum. The size of the produced nodules varied depending on the mentioned parameters. Nodules ranging from 2mm in diameter to 15mm were produced. Smaller nodules crumbled during the clinkering process and proved difficult to collect. After countless attempts and studying the effect of the different parameters on the nodule size, the optimal size was determined to be 5-10mm. To produce these nodules, the machine was set to an rpm of 35 and an inclination angle of 30° (Figure 5). In terms of quantities, 300g of material was added to the granulator, and supplemented with 100mL of water as soon as the drum reached an rpm of 35. The nodules were allowed to form as the drum rotates, and a rubber spatula was used to break the rotation if large clumps formed. Once very

small nodules started forming, water was sprayed onto the powder and left to rotate for a couple of minutes, this caused the nodule size to gradually increase. When the nodules visibly reached the desired diameter range, the machine was stopped, and the nodules were collected. A total of approximately 200mL of water was required for a 300g batch of powder.



Figure 5 Rotating drum granulator



Figure 6 Nodules after clinkering

The nodules were then clinkered in a benchtop Lindberg/Blue-M muffle furnace (Figure 7). The clinkering was done at a temperature of 800-1100°C for 2 hours. The first hour was kept at 800°C to ensure all the organic compounds were burnt off and that all the calcium carbonates had decomposed. The second hour was held at 1100°C to ensure proper clinkering. The reason that this temperature range was chosen is because most industrial MSW incinerators operate at a range of 900-1200 °C. This opens the possibility of recapturing the heat produced by the incinerator to perform the clinkering process in house. The prospect of collecting the raw materials and energy from the same source could provide an avenue towards converting incinerators into a greener Eco-cement production facility.



Figure 7 Lindberg Blue furnace

After clinkering, the nodules were allowed to cool for 24 hours inside the furnace and then pulverized once again to ensure the final product is in fine powder form. The size and shape of the nodules before pulverizing are shown in Figure 6. The entire process of Eco-cement synthesis from raw materials to final product is presented in Figure 8.

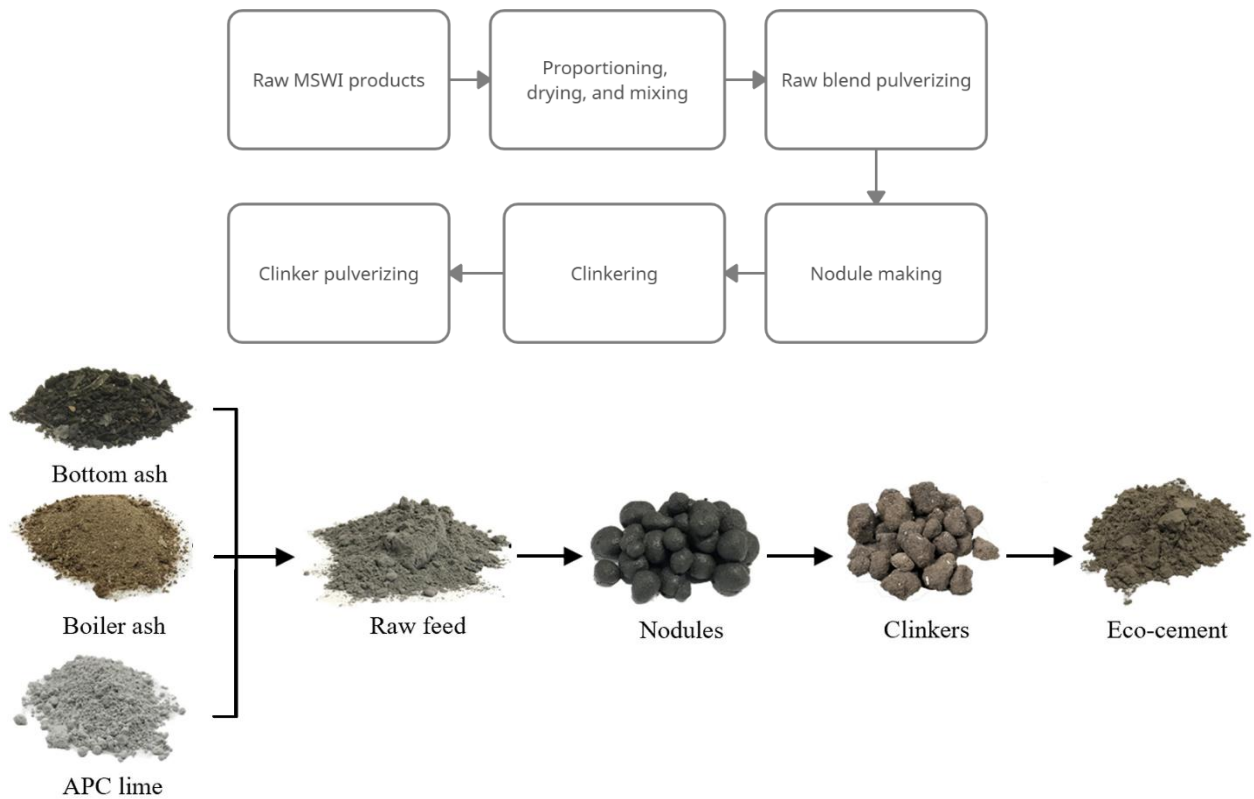


Figure 8 Eco-cement synthesis process

Once the final blend and process were finalized, Eco-cement was mass produced for further testing and validation. A total of 15kg of Eco-cement was prepared in single batches of 1kg. To validate each batch, a small portion of the material was selected using the quartering sampling method. ASTM C702 was used as guidance to ensure that the sampled material was representative of the entire batch. Compressive strength after 28-d hydration was chosen as the validation parameter. Batches that registered a strength lower than 25 MPa were deemed unacceptable and were discarded.

3.4 Characterization of Eco-cement

A Panalytic PW2240 spectrometer was used to perform X-Ray Fluorescence (XRF) analysis on Eco-cement, NewCem, Fly ash, and OPC. Table 7 shows that Eco-cement was found to be high

in SiO_2 , Al_2O_3 , and CaO which are also the main oxides in the other commercial SCMs. These oxides also makeup the majority of normal hydraulic cements.

Table 7 Chemical composition of binders

Oxide	Composition (% wt)			
	OPC	Eco-cement	NewCem	Fly ash
SiO_2	20.54	18.77	36.41	53.81
Al_2O_3	4.57	9.18	11.06	23.16
Fe_2O_3	3.11	3.7	1.13	3.72
MnO	0.1	0.149	0.468	0.046
MgO	2.8	2.68	11.32	1.08
CaO	65	54.33	35.79	10.83
Na_2O	0.24	--	0.89	2.68
K_2O	0.68	< 0.01	0.51	0.69
TiO_2	0.2	2.38	1.04	0.67
P_2O_5	0.26	1.93	0.04	0.11

3.5 Casting procedures

Different replacement percentages were tested to determine the optimal mix design. The results for the 28-day compressive strength are shown in Figure 9. A 25% replacement of OPC by Eco-cement showed the highest compressive strength at 41.2 MPa. However, noticeable inconsistency and cracking was observed for this batch as evidenced by the high standard deviation at this replacement rate. There seemed to be an overbearing differential interplay between the two materials at this rate. Consequently, replacement rate was limited to 15% as this was also the most common cement replacement ratio in the industry for adequate strength.

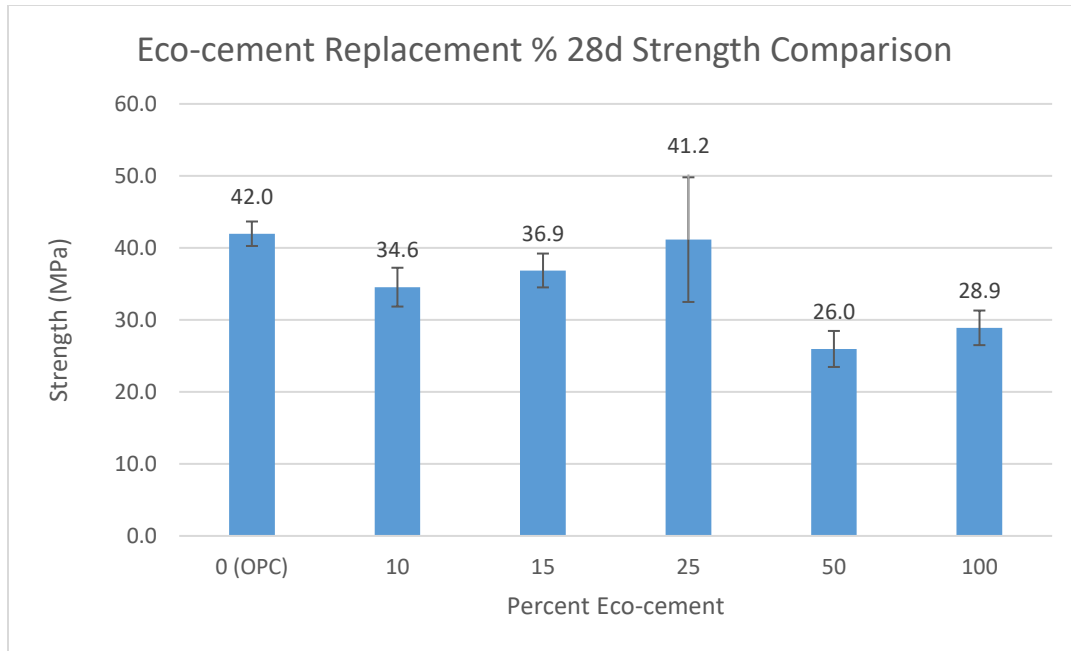


Figure 9 Effect of Eco-cement replacement on 28d strength

All mixes contained 85% OPC and 15% of the tested SCM. The dry powders were mixed for 24 hours using a V rotatory split mixer to ensure homogenous powder distribution. Concrete and paste samples were produced for different tests. The mix proportions are outlined in Table 8.

Table 8 Concrete and paste mix proportions

Blend		Component (% of total)								w/cm ratio
		OPC	Eco-cement	Fly ash	NewCem	Water	SP	Fine aggregate	Coarse aggregate	
Paste compacts	100OPC-P	87	--	--	--	13	--	--	--	0.15
	15ECO-P	74	13	--	--	13	--	--	--	0.15
	15FA-P	74	--	13	--	13	--	--	--	0.15
	15NC-P	74	--	--	13	13	--	--	--	0.15
Concrete	100OPC	19	--	--	--	7.6	0.08	28.6	44.6	0.40
	15ECO	16.15	2.85	--	--	7.6	0.08	28.6	44.6	0.40
	15FA	16.15	--	2.85	--	7.6	0.08	28.6	44.6	0.40
	15NC	16.15	--	--	2.85	7.6	0.08	28.6	44.6	0.40

Paste compacts were produced by mixing the dry powder (85% OPC, 15% replacement SCM) with water at a water-to-cementitious-material (w/cm) ratio of 0.15. For a single specimen, 11g of paste were placed into a cylindrical mold and an MTS machine equipped with a packing rod (Figure 10) was used to apply a 3 kN uniaxial compaction load to produce the compacts. The resulting cylindrical compacts had a diameter of 17 mm and a height of 24 mm. The compacts were then immediately placed in the fog room at 100% relative humidity until the date of testing.



Figure 10 Mold for compact making

Concrete specimens were made by first mixing the dry powders and the aggregates in a traditional bowl mixer for 1 minute. Half of the water was then added, and mixing was continued for another minute. Finally, the remainder of the water and superplasticizer (SP) were added and mixed for 2 minutes. The final mix was poured into 100mm stainless steel cube molds and vibrated using a vibrating table for 45 seconds. The molds were then wrapped in plastic wrap for 24 hours to ensure no moisture was lost during initial curing. The specimens were subsequently

demolded and placed into a fog room set at 100% relative humidity for hydration. Typical concrete and paste samples are shown in Figure 11.

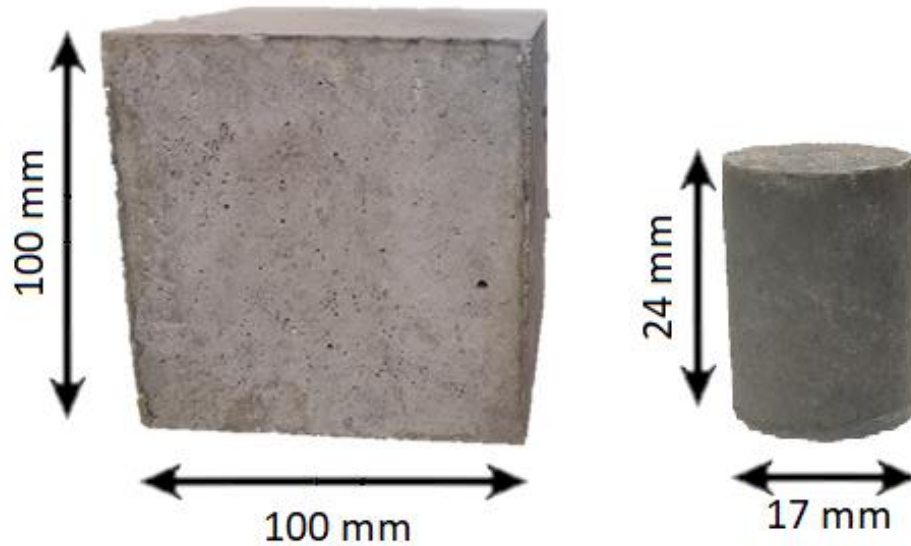


Figure 11 Typical concrete and paste samples

3.6 Testing

The concrete specimens were subjected to multiple tests to fully characterize Eco-cement and be able to draw a fair conclusion when compared to traditional SCMs. Each test was performed on a 100% OPC samples, which served as the reference batch, as well as batches of 15% Eco-cement (15ECO), 15% commercial coal fly ash (15FA), and 15% commercial NewCem GGBFS (15NC). Each batch consisted of 3 samples.

3.6.1 Mineral composition

Quantitative X-ray diffraction (QXRD) analysis was performed on the raw Eco-cement and OPC powders. The powdered samples were mixed with corundum as an internal standard to

estimate the X-ray amorphous content. The test was completed using a Panalytical X'Pert Pro diffractometer along with a Cu X-ray source and an X'celerator detector. The following parameters were used for both samples: voltage: 40 kV; current: 40 mA; range: 5-70 deg 2 θ ; step size: 0.017 deg 2 θ ; time per step: 50.165 sec; divergence slit: fixed, angle 0.5°. The X'Pert HighScore Plus software was used to identify the crystalline mineral phases using the PDF-4 Minerals ICDD database. The quantities of the crystalline minerals were determined using the Rietveld method.

Scanning electron microscope (SEM) was used to examine the composition of the raw Eco-cement powder. The powder was coated in a 5 nm layer of platinum to improve conductivity and an FEI Inspect F50 FE-SEM was used to perform the analysis. Dispersive X-ray spectroscopy (EDS) was also utilized to detect the elemental composition of the targeted regions.

Finally, due to Eco-cement containing MSWI residues, it was important to evaluate the final product from an environmental standpoint. A toxicity characteristic leaching potential test (TCLP) was performed to determine the concentration of heavy metals in the resulting leachate solution. The test was performed in accordance with TCLP method 1311 by the United States Environmental Protection Agency (EPA). The test was performed on 28-day hydrated concrete cube that was crushed using a jaw crusher to particle sizes averaging 9.5 mm in diameter. The concrete was placed in an extraction solution and mixed at 30 rpm for 18 hours. The final solution was then used in the TCLP test using the acid digest method.

3.6.2 Compressive strength, setting, and hydraulic performance.

Compressive strength testing was done in two stages. First, paste samples were tested after 1, 28, 60, and 90 days of hydration and in accordance with ASTM C39. This was done to

evaluate the performance of Eco-cement on a smaller scale, without the effect of aggregates. Testing was done using a SINTECH 30/G MTS machine with a 150kN load cell at a rate of 0.5 mm/min (Figure 12).



Figure 12 MTS Sintech 30/G - Compact testing

Once the paste samples showed promising results. Concrete specimens were prepared and tested at hydration ages 1, 28, 60, and 90 days as per ASTM C39. Testing was performed using an MTS Series 315 Load Frame (Figure 13), connected to a FlexTest 40 digital controller. The strain rate was set to 0.11 mm/min.



Figure 13 MTS Series 315 - Concrete testing

The workability of fresh concrete was evaluated using a Vicat needle (Figure 14) in accordance with ASTM C191. Each mix was combined with different water ratios to achieve the same starting standard paste consistency. The Vicat needle was then dropped onto the surface of the paste every 15 minutes until the needle penetration was limited to less than 25 mm (initial time of setting). The testing was continued until the needle no longer left a circular imprint on the surface (final time of setting).



Figure 14 Vicat needle apparatus

Isothermal calorimetry was performed on the specimens to measure the heat of hydration in accordance with ASTM C 1679. The procedure was performed using a water to binder ratio of 0.4 at 20°C. Measurements were taken using a TAM Air 8-channel.

Standardized cementitious and pozzolanic tests were performed to see under which category Eco-cement fits. For the pozzolanic test, 50 mm cube mortar samples were prepared in accordance with ASTM C593. This test indicates a hydrated lime ($\text{Ca(OH}_2\text{)}$) to SCM ratio of 1:2. Eco-cement was compared to commercial pozzolanic Class CI Fly ash . Curing was completed in a sealed container at 100% relative humidity and placed in an oven at 54° for 7 days. To keep the humidity levels high, water was sprayed on the inside of the container twice a day. The compressive strength was tested after curing.

The ASTM C989 cementitious test was similarly carried out on 50 mm mortar cube samples with a 1:1 OPC to SCM ratio. NewCem was the commercial reference material employed for relative comparison. The samples were submerged in lime water for curing for a duration of 7 days.

3.6.3 Pore structure analysis and durability testing

Surface resistivity is a very useful non-destructive test for concrete, having an inverse correlation to the porosity and void structure of concrete – less porous materials yield higher resistivity values (Coppio, et al., 2019). Testing was carried out according to AASHTO T358 using a digital Resipod Proceq Resistivity meter (Figure 15). Cubic concrete samples at ages 1, 28, 60, and 90 days were used. The meter recorded resistivities along the diagonals of the cubes and for all faces. Measurements were averaged and recorded.



Figure 15 Resistivity meter and calibration board

Another parameter that provides insight into the void structure of the concrete is water absorption. The test was performed in accordance with ASTM C642. Weight readings for concrete specimens were taken at three stages: after oven drying, after water submersion, and after 7 hours of boiling. For each scenario, readings were recorded for over 24hrs and until the weight change between readings was less than 0.5%. These measurements along with the suspended weight in water were used to calculate the volume of voids in the concrete.

The freeze/thaw durability of concrete has a strong correlation with its pore structure. Different factors such as pore size, volume, and distribution have a direct effect on the freeze/thaw resistance of concrete (Cai & Liu, 1998). Concrete in the field is subjected to freeze thaw cycles every winter. These cycles can quickly add up and cause major scaling, microstructure breakdown, and decrease in strength (Chen & Shi, 2019). Freeze/thaw resistance was measured in accordance with ASTM C672. 28 day hydrated concrete samples were subjected to freeze/thaw cycling while fully submerged in a de-icing salt solution. The solution contained 4g of Sodium Chloride per 100mL of water. The samples were frozen for 16-18hrs and then allowed to thaw for 6-8hrs in the set up presented in Figure 16. After every 5 cycles, the scaled pieces of concrete were collected, fully dried at 105°C, and weighed to determine the mass loss. The final mass of the concrete blocks was also recorded at the end of the test. This was used to determine the cumulative mass loss of the concrete samples.



Figure 16 Thawing (top) and freezing (bottom) set up

4 Results and Discussion

4.1 QXRD of Eco-cement

Table 9 QXRD of Eco-cement and OPC

Mineral	Formula	Wt (%)	
		Eco-cement	OPC
C2S	Ca_2SiO_4	46.1	19.9
C3S	Ca_3SiO_5	n.d	47.8
Tricalcium aluminate	$\text{Ca}_3\text{Al}_2\text{O}_6$	n.d	4.5
Wadalite	$\text{Ca}_6\text{Al}_5\text{Si}_2\text{O}_{16}\text{Cl}_3$	16.9	n.d
Chlorellestadite	$\text{Ca}_{10}(\text{SiO}_4)_3(\text{SO}_4)_3\text{Cl}_2$	6.8	n.d
Portlandite	$\text{Ca}(\text{OH})_2$	2.5	n.d
Periclase	MgO	2.2	1.4
Quartz	SiO_2	n.d	0.3
Calcite	CaCO_3	n.d	1.6
Gypsum	$\text{CaSO}_4\cdot 2\text{H}_2\text{O}$	n.d	1.5
Brownmillerite (C4AF)	$\text{Ca}_2\text{FeAlO}_5$	n.d	8.1
Amorphous		25.5	15.0

n.d: Not detected

According to the QXRD results shown in Table 9, the most abundant minerals in Eco-cement were found to be C_2S (Belite), Chlorellestadite (CE), and Wadalite. C_2S was expected to be the mineral with the highest abundance due to the relatively low clinkering temperature. Eco-cement was designed to promote the formation of reactive C_2S as it is a common hydraulic phase in OPC. Chlorellestadite and Wadalite make up 24% of Eco-cement, both of which molecularly entrap chlorine. CE is a relatively new literary addition to the ellestadite group consisting of silicate-sulfate apatites. Literature shows that CE rarely occurs in nature, but similar formations can be found as intermediate high-temperature phases in Portland clinker and burned coal spoil-heaps. CE is formed at 965–1165 °C which is the same range in which Wadalite is formed. These two minerals often form together (Środek D. , et al., 2018), and this trend is also observed in Eco-cement. Figure 17 shows the diffraction pattern of Eco-cement.

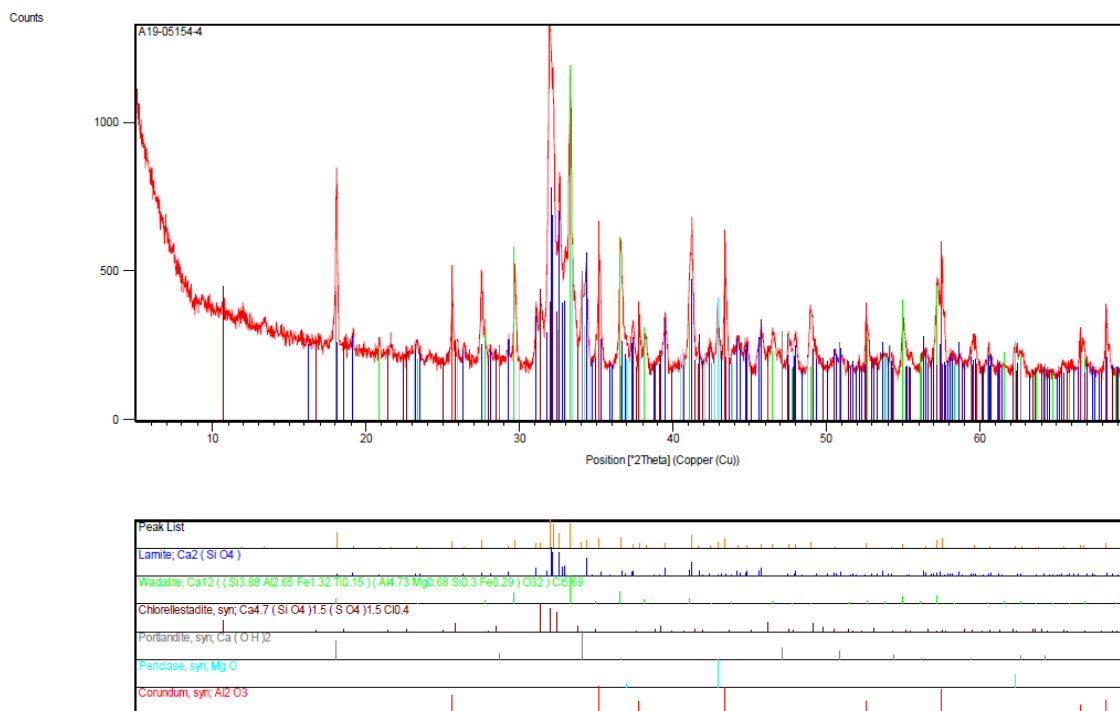


Figure 17 QXRD diffraction pattern for Eco-cement

4.2 SEM

To further investigate the presence of CE in Eco-cement, SEM was used on the raw powder. EDS was employed to indicate the CE crystals and determine their chemical composition as calcium, silicon, oxide, sulfur, and chlorine (Figure 19). CE crystals seen in Figure 18 were observed to be longitudinal hexagonal crystals as described in the literature (Saint-Jean, et al., 2005; Śródek, et al., 2018; Zhang, et al, 2020).

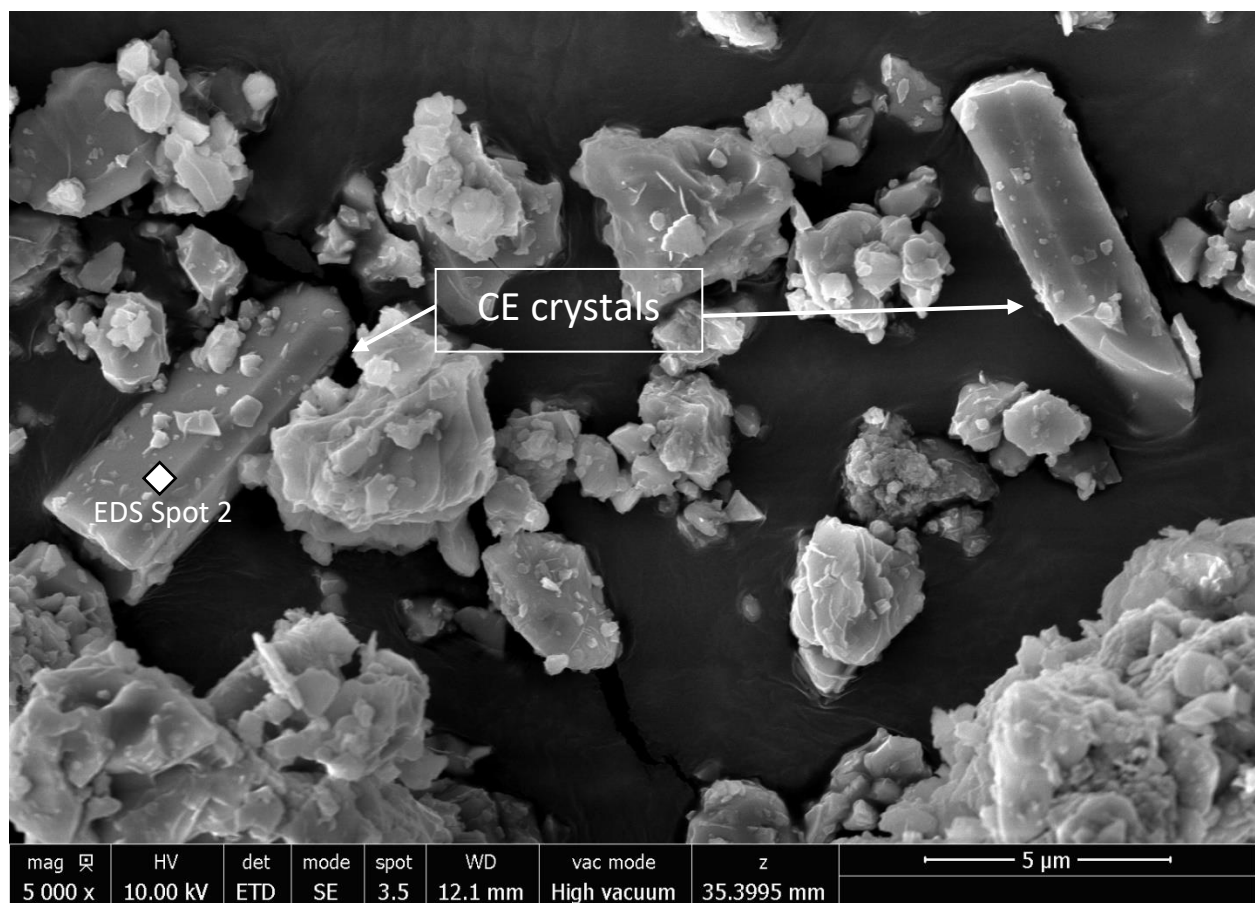


Figure 18 SEM of raw Eco-cement

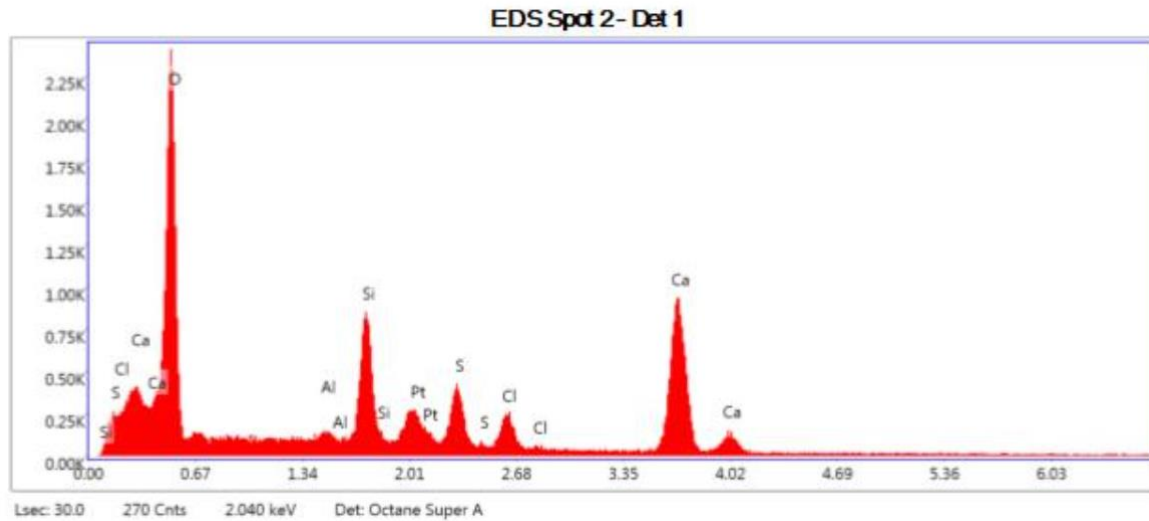


Figure 19 EDS of raw Eco-cement

4.3 Compressive strength

Compressive strength is arguably the most important test when appraising a cementing material. Testing the compressive strength of paste compacts served as the very first indication of whether Eco-cement has further potential to be explored. Testing paste specimens also removed the uncertainty and inconsistencies otherwise introduced by aggregates, this allowed the focus to be fully on the binder's hydration. The compressive strength results for paste compacts for multiple hydration durations are shown in Figure 20.

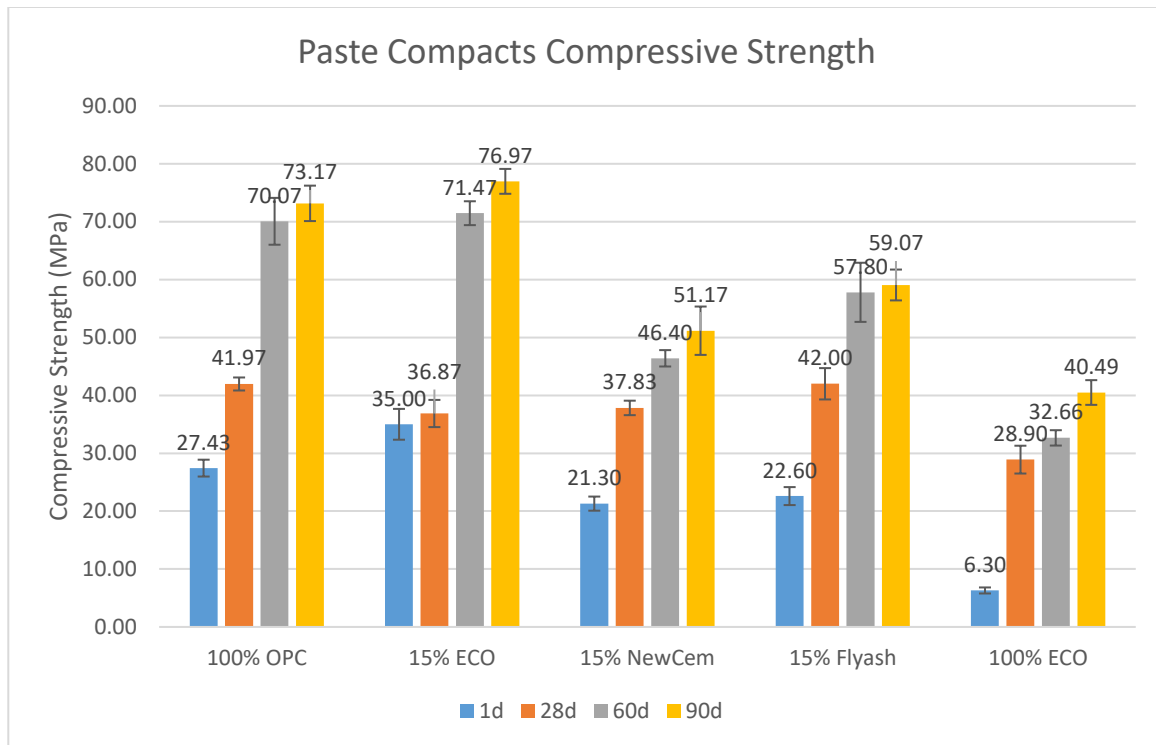


Figure 20 Paste compacts compressive strength

The 15% ECO samples immediately stand out due to their high ultimate strength, achieving the highest 90-day value, which was 5% higher than the same-age straight OPC paste specimens. More interestingly, however, the 1-day strength of 15%ECO recorded a 28% increase over OPC paste, implying a sort of accelerator effect associated with the Eco-cement blend. This may very likely be due to the high chlorine content in Eco-cement. Chlorine-based additives have well established uses in accelerating the hydraulic reaction of cement. Calcium chloride (CaCl_2) for example is a very popular commercial accelerator. CaCl_2 increases the dissolution and hydration rates of the calcium-silicate components of cement, particularly the C_3S – alite phase mainly responsible for early age strength (Kipkemboi, et al., 2020). The addition of CaCl_2 usually results in a 50% increase in the rate of OPC's early strength-gain. This gain is directly proportional to the amount of CaCl_2 supplementation but only up to a certain threshold, above which ultimate

strength will be undermined. The recommended dosage is around 2% the weight of OPC (Ramachandran, 1996). Eco-cement, however, does not seem to suffer from the same caveat as traditional CaCl_2 . This waste-derived additive provides a comparatively lower acceleration rate (28% vs 50%), but its relatively higher dosage does not decrease the ultimate strength of the OPC blend.

The commercial benchmark control additives, Fly ash and NewCem, did not promote any significant early age or ultimate strength for the paste specimens. This is likely due to the lack of aggregates. In normal concrete, the interfacial transition zone (ITZ) around aggregates is a point of weakness and high porosity due to the “wall effect”. In this zone, a water concentration gradient forms around the aggregate leading to a localized increase in w/cm ratio and lower strength than the bulk of the paste (Ollivier, et al., 1995). GGBFS and Fly ash have been found to densify the ITZ zone and provide a better mortar-aggregate interlock and thereby increase the overall concrete strength (Duan, et al., 2013; Shaban, et al., 2021). The lack of aggregates and ITZ therefore greatly reduces the effectiveness of these SCMs. The different pore size distribution in paste vs concrete may also be a factor in the reduced success of Fly ash and NewCem.

Figure 20 reveals that the 100% Eco-cement specimens also registered some notable latent hydraulic behaviour, reaching strengths of 30 MPa in 28 days, and 40 MPa in 90 days. This is an indication that Eco-cement exhibits some cementitious properties. This promising hydraulic effect along with the increase in early age and ultimate strength demonstrated by the 15%ECO compacts warranted that further testing be carried out on concrete specimens as the next step of the validation process. Figure 21 shows compressive strength results obtained for the concrete specimens.

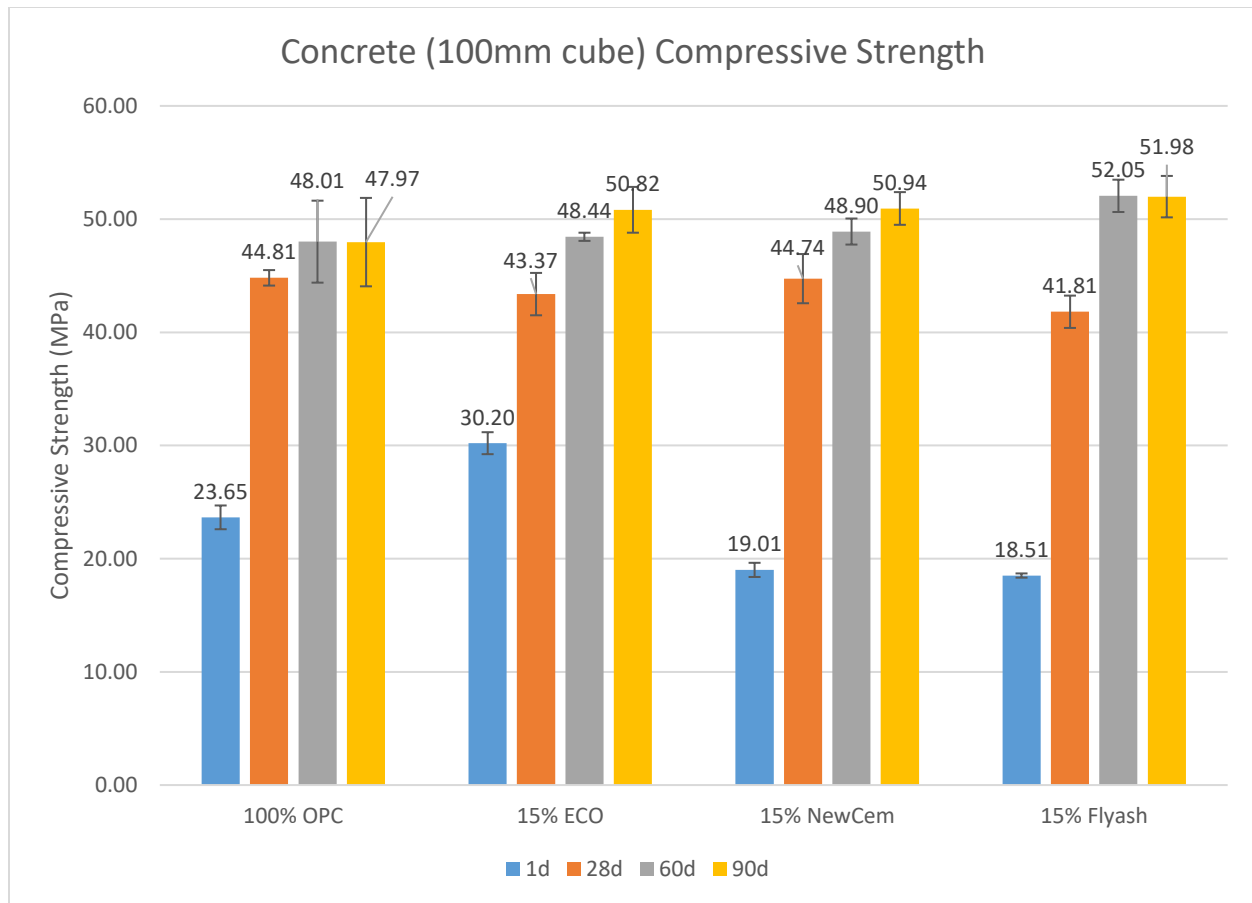


Figure 21 Concrete compressive strength

In line with the paste results, 15% ECO concrete samples also showed a steep increase (28%) in 1-day compressive strength compared to Portland concrete control batch. This phenomenon was only observed in the Eco-cement samples. Fly ash and NewCem blended concrete batches did not contribute to early age strength, but rather expectedly recorded lower 1-day strength values than the control batch. The ultimate strength was almost identical for the three tested SCMs, where the respective batches were all higher than the control batch and plateaued around the 51 MPa mark after 90 days.

4.4 Setting time

The Vicat needle method was used to determine the time of setting of the control and blended paste samples. A plot of penetration depth against time is shown in Figure 22 for all four samples. In line with the rapid strength gain effect observed in Section 4.3, the Vicat needle test also showed that the Eco-cement blended paste achieved the fastest setting. Despite NewCem starting to show hardening 30 minutes before Eco-cement, the high setting rate of Eco-cement allowed it to make up the difference, reaching 0 mm penetration 30 minutes before the NewCem blend. On the flipside, Fly ash demonstrated the slowest setting time, starting to harden almost an hour after OPC and reaching a final setting time well after all the other specimens. This is to be expected as fly ash being a pozzolan has a retardation effect, and the benefits of adding a pozzolan to a cement mixture do not appear until later in the hydration process (Fantu, et al., 2021).

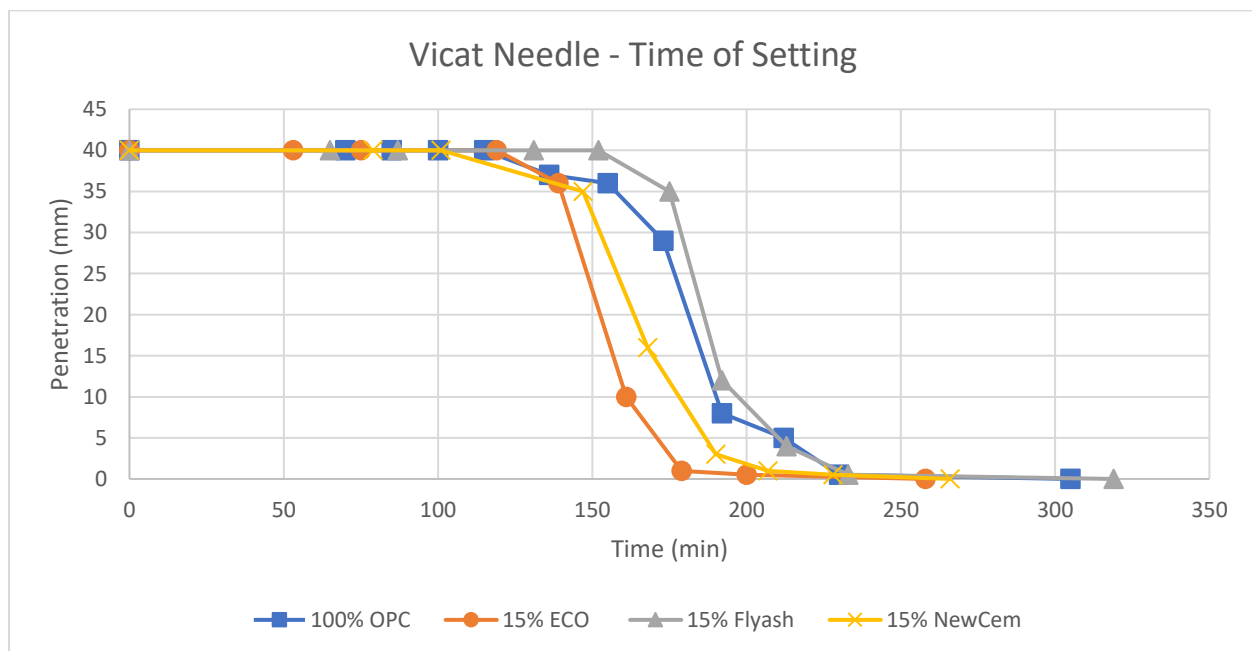


Figure 22 Vicat needle setting rate

Figure 23 shows the initial (25 mm penetration) and the final (0 mm penetration) of the specimens. As expected, Eco-cement reduces the initial and final setting time of concrete by 16% and 15%, respectively. These results support the theory that the high chlorine content in Eco-cement allows it to act as an accelerator in the first 24 hours of hydration.

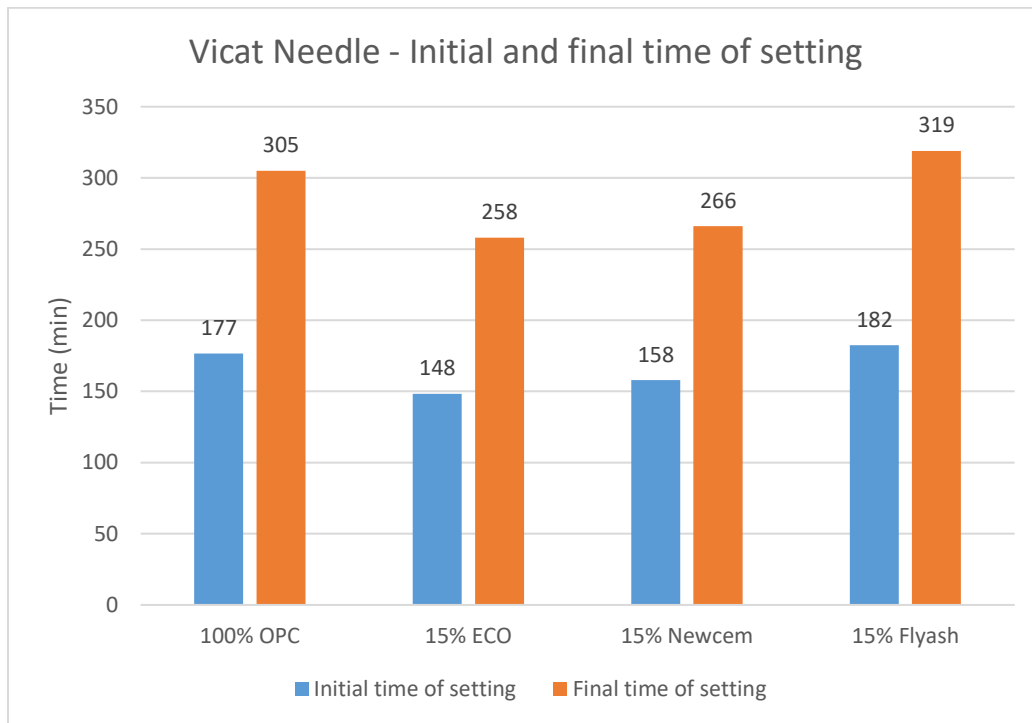


Figure 23 Vicat needle initial and final time of setting

4.5 Heat of hydration

Heat of hydration calorimetry was used to further understand the behaviour of Eco-cement, particularly in the first hours of the hydration reaction. Tests were performed on straight 100% OPC, as well as 50% and 15% Eco-cement replacement samples. The results of the heat flow per gram of solid are shown in Figure 24.

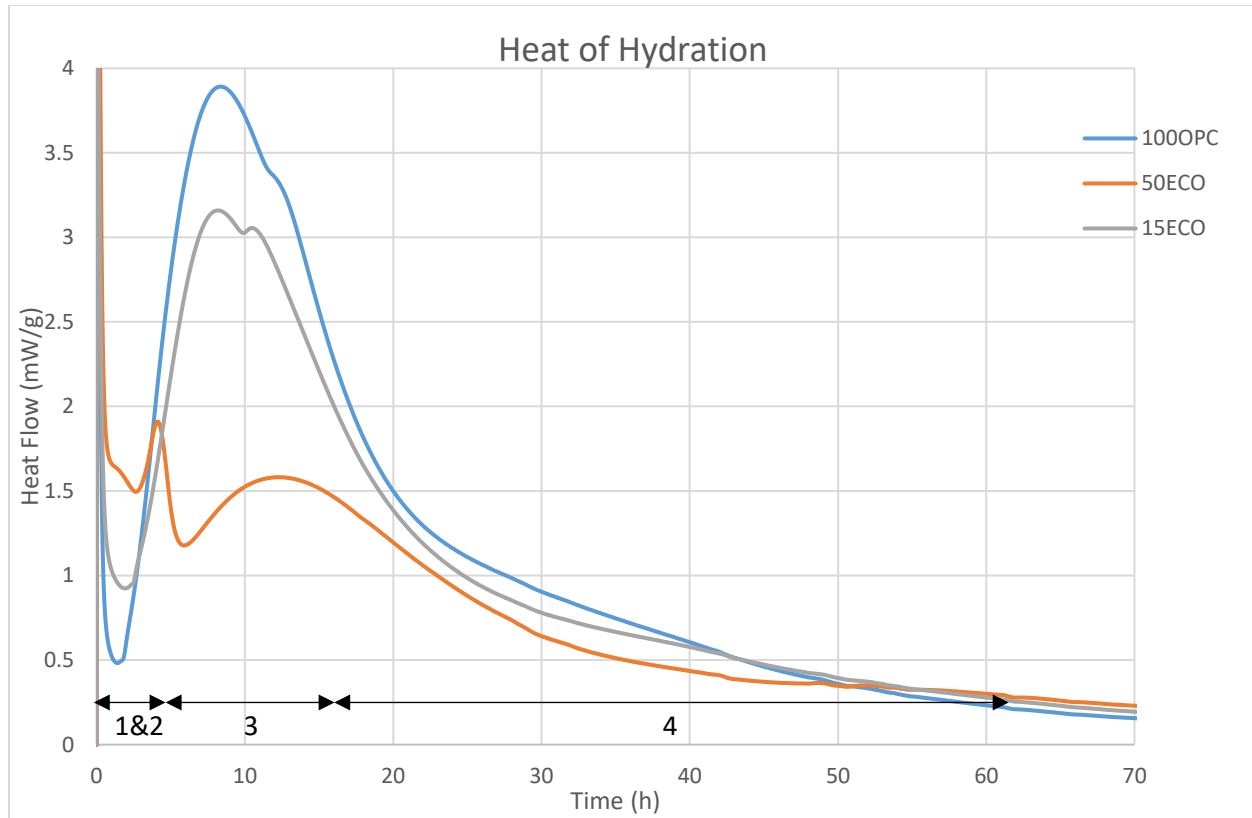


Figure 24 Heat of hydration results

100OPC: 100% OPC

50ECO: 50% Eco-cement, 50% OPC

15ECO: 15% Eco-cement, 85% OPC

The results can be interpreted in four separate reaction stages. Stage 1 is the induction period and occurs at the very beginning of the reaction, represented by a very high peak. The heat released during this period is due to the initial contact of the cement particles with water and the dissolution of the cement as some hydration reactions begin. The main source of heat in this stage is the exothermic dissolution of C_3S (Bullard, et al., 2011). The short time after the induction stage is called the dormant period and is distinctively recognized by the low heat flow (stage 2). Stage 3 is the acceleration phase, during which substantial amounts of the calcium-silicate component of cement (mainly C_3S) engages in hydraulic reaction to form hydration products C-S-H and CH (Wang, et al., 2021). The shoulder effect represented by a second peak

during stage 3 is likely due to an irregular set regulation which leads to an imperfect chemical reaction where a delayed formation of ettringite or gypsum is observed. (Bensted, 1987). Stage 4 is the final phase when the reaction is mostly complete and has stabilized. This is known as the deceleration and hardening period.

Looking at stage 2 (Figure 25), the higher reaction heat detected during 50% Eco-cement replacement fits well with the acceleration effect observed in the compressive strength and time of setting results. During this dormant period, an impermeable ettringite layer is usually formed around the hydrated cement particles which causes a temporary stop in the hydration reaction (Hekal & Kishar, 1999; Sauvat, et al., 1999). The high chlorine content in Eco-cement is presumed to react with the C_3A to form hydrochloroaluminate instead of ettringite. This is a much more soluble material and allows for the reaction to proceed faster, explaining the acceleration effect (Sauvat, et al., 1999). Furthermore, the observation of multiple peaks in the 50% Eco-cement sample is another indication of early setting as some chemical reactions continue to occur after the first peak. This happens due to an irregular hydration process which can cause multiple subsequent reactions such as the formation of dihydrate gypsum from calcium sulphate hemihydrate hydration (Bensted, 1987).

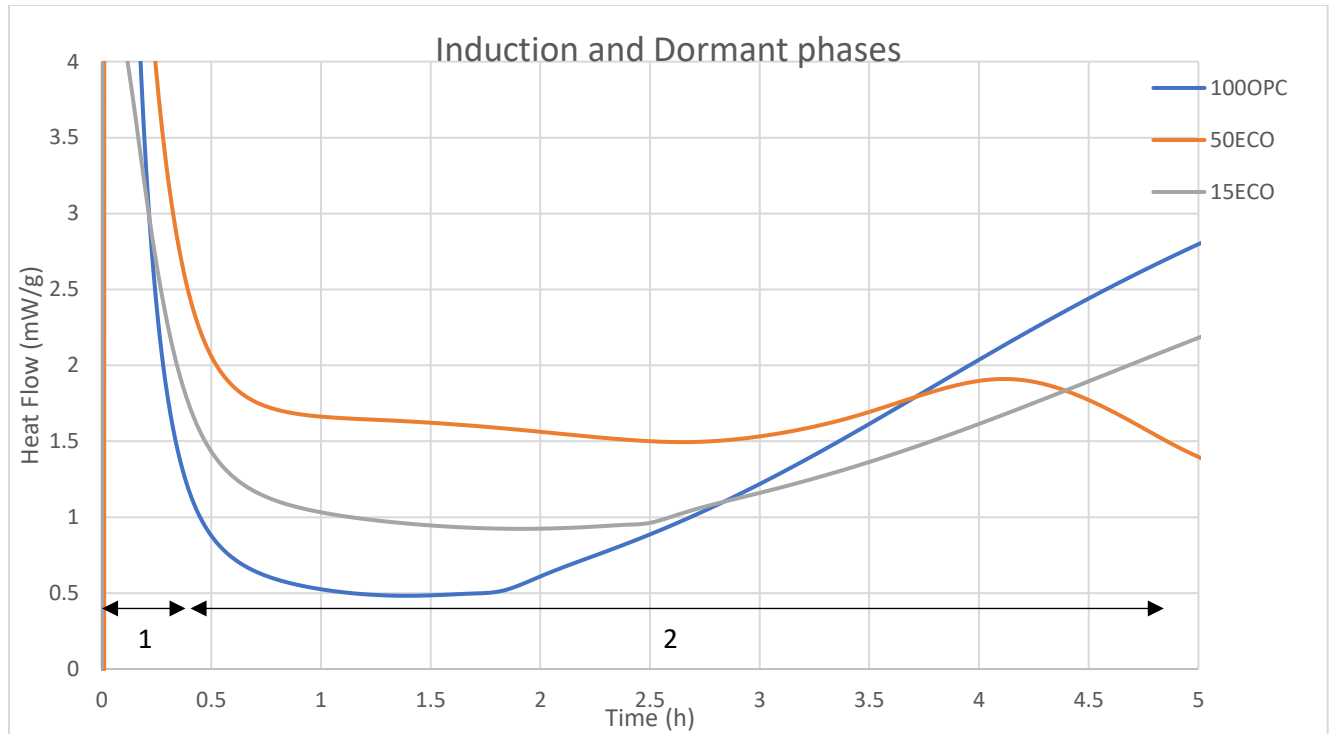


Figure 25 Induction (1) and dormant (2) stages

Figure 25 shows a close up of stage 1 and 2 of the reaction. The combined duration of these stages is approximately 5 hours. This matches almost exactly with the final time of setting from the Vicat needle test (300 min) seen in Figure 22. During this period, the cement paste has not yet hardened and is still relatively soft. The much higher reaction heat generated by high Eco-cement replacement levels could be a catalyst for differential thermal expansion between the OPC and Eco-cement, which leads to cracking. The addition of cementitious materials such as GGBFS has also been linked to early age cracking due to a similar temperature gradient (Schutter, 1999; Schutter & Taerwe, 1995). This phenomenon can also be seen in the strength results of the 50% Eco-cement replacement samples shown in Figure 9. When OPC was replaced with 50% Eco-cement there was a sharp 40% decrease in compressive strength. This can be visually seen in Figure 26 where 50% Eco-cement specimens show significant cracks down the radial diameter

even before compressive testing was carried out. The position of the cracks is likely due to the nature of the two-part mold. During demolding the two sides of the mold are slightly pulled apart which causes a weaker plane in the middle of the sample.



Figure 26 Cracking in 50%ECO paste samples

During stage 3 (Figure 24), it can be seen that 15%ECO closely shadowed the 100%OPC curve, while a higher replacement rate in the 50%ECO samples showed a drastic reduction in the heat flow. The acceleration period represents the most important hydration processes in concrete: the silicate reaction to form C-S-H (Schöler, et al., 2017). Because Eco-cement contains fewer overall silicates (C_5S and C_3S) than OPC, a lower heat generation is expected with higher replacement rates. This dilution effect is clearly observed in the heat of hydration results.

4.6 SCM classification

It is good practice to classify SCMs into their appropriate categories. Going by the increased compressive strength of Eco-cement blended concrete, a logical first step is to test for cementitious and pozzolanic behaviour as these are indicative mechanisms that are known to contribute to ultimate strength.

To test for pozzolanic behaviour, ASTM C593 was followed. SCMs in this test are mixed with hydrated lime in a ratio of 2:1 and cured at 54 °C. The results are presented in Table 10. As

expected, Fly ash performed exceptionally well, reaching 7.3 MPa. Eco-cement on the other hand did not meet the minimum strength requirement, recording a compressive strength of only 1.7 MPa. Another indication to the lack of pozzolanic activity in Eco-cement is early age strength; Eco-cement had conversely shown accelerated 1 day strength gains in both paste and concrete specimens, while pozzolans are known for their delayed contribution to strength gain (Fantu, et al., 2021).

Table 10 Pozzolanic activity results

SCM	Strength (MPa)
Fly ash	7.3
Eco-cement	1.7
Minimum required strength ^a	4.1

a: ASTM C593

The results from the cementitious test (ASTM C989) are shown in Table 11. In this test, the SCM represents 50% of the total binder with the other half being straight OPC. NewCem is a known cementitious material and performed just as expected with a strength index of 0.82, well above the minimum specified by the standard. Eco-cement fell short at a strength index of 0.46. This was expected due to the high replacement rate which was linked to reduced compressive strength and cracking as shown in previous sections.

Table 11 Strength Index of cementitious test

SCM	Strength (MPa)	Strength Index
100% OPC	19.5	1.00
Eco-cement	9.0	0.46
NewCem	16.0	0.82
Min. Strength Index ^a		0.70

a: ASTM C989

Despite underperforming in the cementitious test, it is still possible that Eco-cement is a cementitious material, or at least behaves similar to one. This is evident by the observed hydraulic activity in pure Eco-cement paste compacts reaching 31 MPa (Figure 20) and the high C_2S mineral content (Table 9). The 50% loading rate instructed by the standard seemed to exceed the limit beyond which point the differential hydration behavior becomes destructive for this hybrid OPC/Eco-cement binder system.

4.7 Water absorption

Water plays an important role in almost all the deterioration mechanisms in concrete whether it be a direct contributor in frost damage and shrinkage cracking, or a carrying medium for chemical deterioration such as chloride ion erosion (Zhao, et al., 2021). Another major cause of deterioration enabled by water is steel reinforcement corrosion. With this direct link between water seepage into the concrete and deterioration, it is imperative that the flow of water into the concrete be studied extensively. The water absorption test proposed in ASTM C642 allows us to explore the outcomes of adding different SCMs to the concrete mix and studying the effect on the absorption.

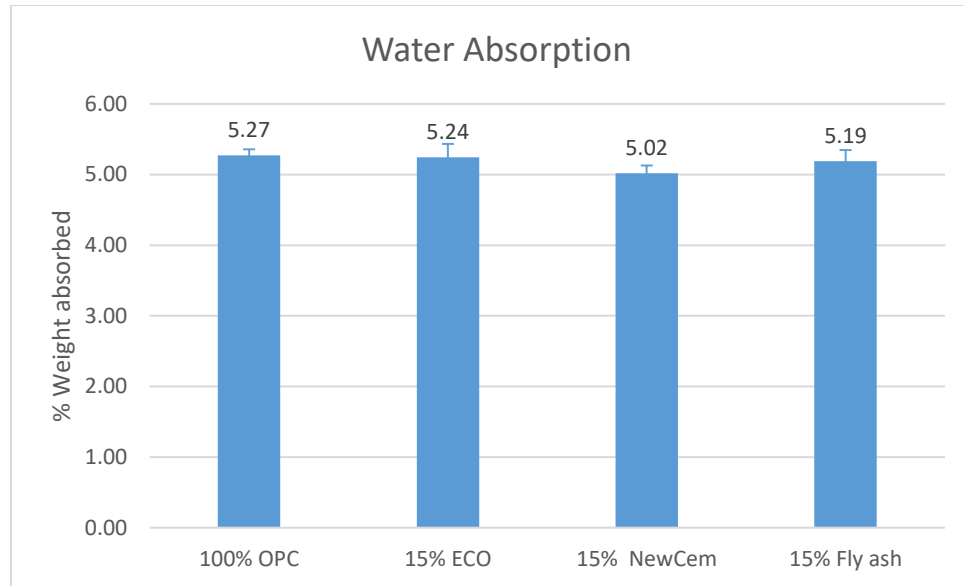


Figure 27 Water absorption results for concrete specimens

Results from the water absorption test are shown in Figure 27. Water absorption after submersion did not seem to be affected by the type of SCM in the concrete with all values being within 4% of each other. After the absorption had been recorded, the specimens were boiled for 7 hours and the submerged weight in water was determined. The volume of voids could then be calculated using the following formula (ASTM C642):

$$Volume\ of\ voids = \frac{A - B}{A - C}$$

Where:

B = mass of oven-dried sample in air, g

A = mass of surface-dry sample in air after immersion and boiling, g

C = apparent mass of sample in water after immersion and boiling, g

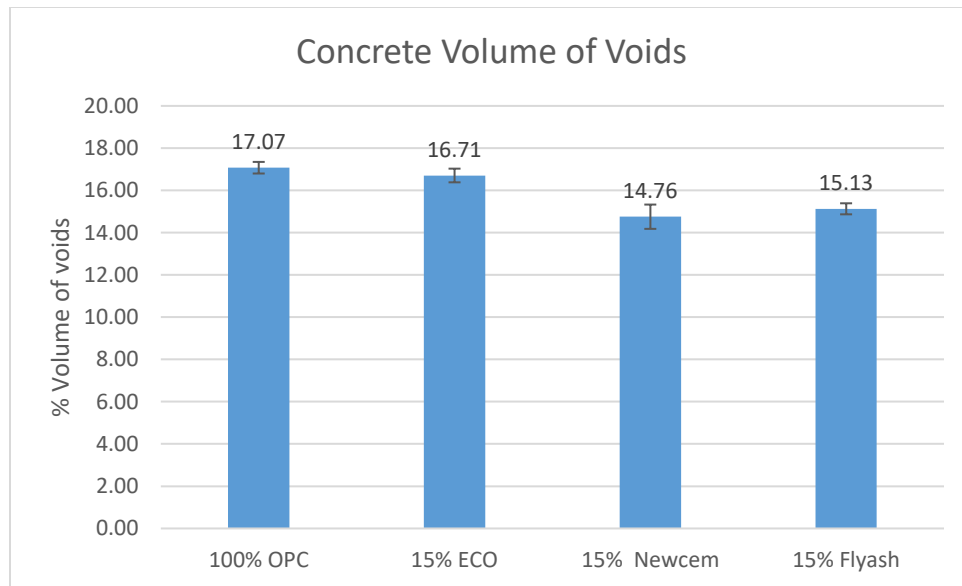


Figure 28 Concrete volume of voids

The volumes of permeable pores turned out to be more revealing and are presented in Figure 28. Eco-cement blends showed just a slight reduction in the volume of voids compared to straight OPC concrete, with both sitting around 17%. NewCem and fly ash both showed a more significant reduction of 13.5% and 11.4% respectively. These values correspond well to the absorption test (Figure 27) where high absorptions coincided with higher volume of voids. The volume of voids also directly correlate to compressive strength (Figure 21) as expected, where a lower volume of voids represented a higher compressive strength.

4.8 Surface resistivity

Surface resistivity is another test that lends insight into the relationship between concrete surface porosity and water retention. The test works by running a current through the concrete and detecting it at different points along the concrete surface. Water is an electrical conductor, meaning that the higher volume of water filling the voids in the concrete the more current will pass through. This leads to an inverse relation where a higher resistivity means that the concrete

is less porous and therefore less prone to absorb water. The surface resistivities for the four different concrete batches are varying ages are shown in Figure 29.

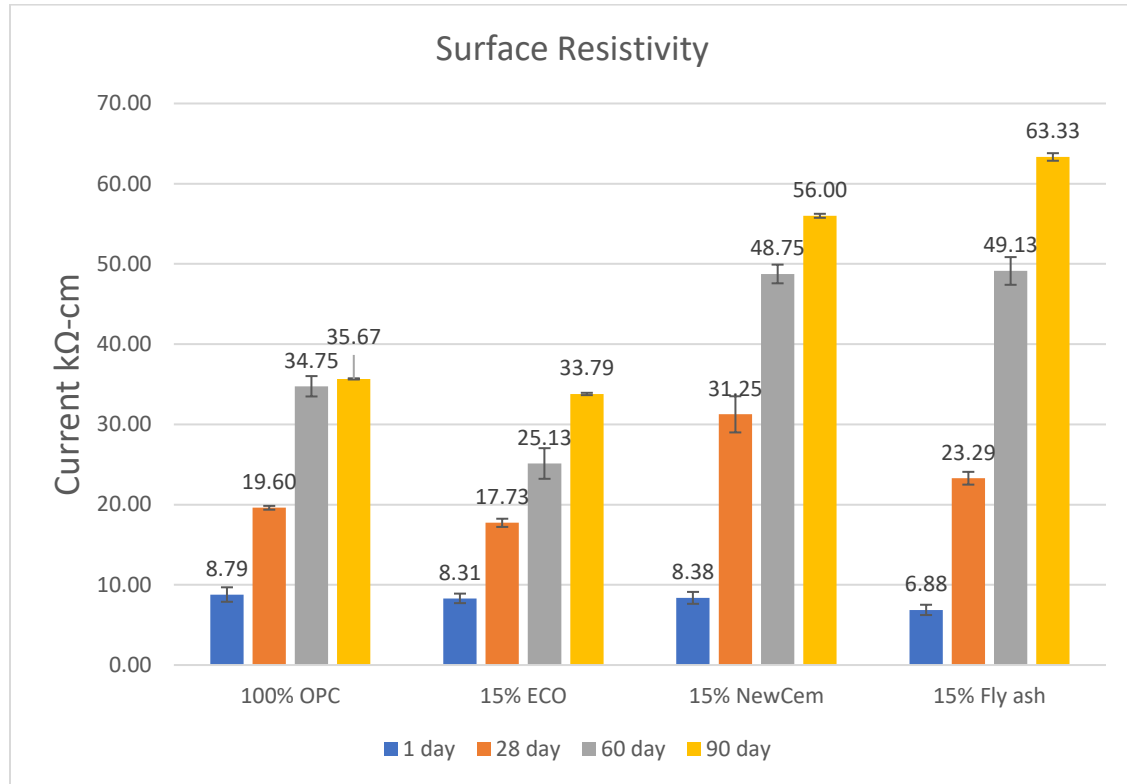


Figure 29 Surface resistivity results

The gradual increase in surface resistivity with hydration age is an expected outcome as the cement reacts and forms more hydration products, filling the pores in the concrete and reducing the electrical flow. Fly ash and NewCem showed very high resistivity by the 90-day hydration mark, reaching 56 and 63 kΩ-cm, respectively. This matches the results seen in the literature where NewCem and fly ash consistently improve the surface resistivity of concrete (Chidiac & Shafikhani, 2020; Duran-Herrera, et al., 2019). The surface resistivity results for NewCem and fly ash are also in line with the reduced volume of voids observed in section 4.7 (Figure 28).

In contrast, the concrete batch prepared using Eco-cement did not perform as well as NewCem and fly ash. At 90 days of hydration, the batch Eco-cement recorded an average surface resistivity that was in fact lower than that of the control OPC by 5%. The most likely reason for this is the change in the ionic concentration of the pore fluid, which is a known parameter that affects surface resistivity (Porrás, et al., 2020). The high content of chlorine containing minerals and salts in Eco-cement provide Cl⁻ ions that dissolve in the water, creating a more conductive medium that allows a larger current to pass through. This phenomenon is observed in other chloride containing admixtures such as accelerators and water reducers (Ahmad, 2003; Pruckner & Gjorv, 2004; Yousuf, et al., 2020). Eco-cement likely alters the conductivity of the pore fluid, thus making the comparison between the concrete batches experimentally inconclusive.

4.9 Freeze/thaw

The results from the freeze/thaw testing are shown in Figure 31. At 100 cycles of testing, all of the samples remained relatively unaffected, retaining more than 96% of their mass. Eco-cement does not seem to have any negative effects on freeze/thaw resistance in concrete, with all samples showing results within 1% of each other. These observations are in line with findings in the literature where blended and straight Portland concrete experienced weight loss of less than 5% at 100 cycles (Mu, et al., 2002; Richardson, et al., 2011; Shang & Yi, 2013). At this testing age, all of the samples experienced small amounts of surface scaling (Figure 30).



Figure 30 Typical concrete cube at 100 freeze/thaw cycles

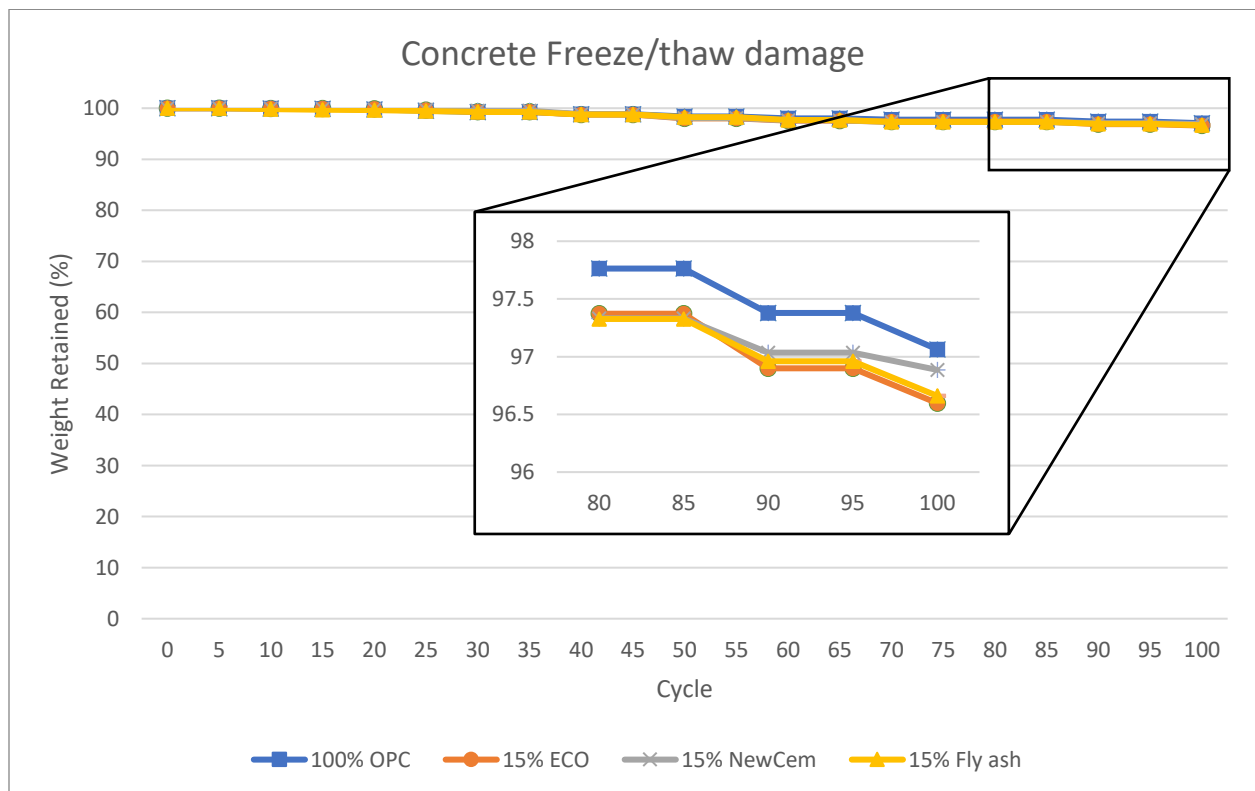


Figure 31 Concrete freeze/thaw results

4.10 Leaching

Due to the toxic nature of MSWI residues used in Eco-cement, it was necessary to determine the effectiveness of stabilizing the heavy metals via clinkering. Ten heavy metals were targeted by the TCLP test and measured concentrations were compared to Canadian and U.S health standards. Along with the heavy metals, the content of Cl^- in Eco-cement was also determined. The leaching test evaluates the performance of Eco-cement under the worst-case scenario, where concrete is crushed into small granules and immersed in a strong extraction solution. These testing conditions are extreme and not representative of real service life. The results presented in Table 12 show that Eco-cement was well below the limit for all heavy metals and Cl^- showing that Eco-cement is stabilized through clinkering and is safe for use as an additive in concrete.

Table 12 Heavy metal leaching performance

Parameter		Eco-cement [mg/L]	Canada, Ontario Regulation 558 ^a [mg/L]	U.S. EPA Regulation ^b [mg/L]
Arsenic	As	<0.02	2.5	5.0
Barium	Ba	0.25	100.0	100.0
Boron	B	0.19	500.0	–
Cadmium	Cd	<0.001	0.5	1.0
Chromium	Cr	0.13	5.0	5.0
Lead	Pb	<0.01	5.0	5.0
Mercury	Hg	<0.001	0.1	0.2
Selenium	Se	<0.01	1.0	1.0
Silver	Ag	<0.01	5.0	5.0
Uranium	U	<0.01	10.0	–
Chloride	Cl^-	11.4	–	230/860 ^c

a: Canada Ontario regulation 558/00: General-waste management.

b: U.S. EPA 40 CFR 261.24 – Toxicity characteristic for heavy metals.

c: U.S. EPA Ambient water quality criteria for chloride – 230 mg/L for chronic freshwater; 860 mg/L for acute freshwater.

5 Conclusions

This work demonstrated that Eco-cement can be produced from 94% MSWI residues with a supplementation of only 4.9% CaO and 1.47% SiO₂. Eco-cement was devised to use all the residues available at a local incinerator (bottom ash, boiler ash, and APC), solving a major environmental concern. Due to the relatively low clinkering temperature of 1100 °C, C₂S was the most prominent hydraulic phase in Eco-cement. Eco-cement blends were designed with a focus on increasing the formation, hydration, and stabilization of C₂S, mainly by altering the percentage of available TiO₂. QXRD determined that the main clinkering products of Eco-cement were C₂S, Wadalite, and Chlorellestadite, the latter two containing significant amounts of Cl⁻ and accounting for 24% by weight of the active phases.

Evaluation of Eco-cement as an additive to commercial OPC was performed. An industry standard replacement rate of 15% was used to perform strength and durability testing. Eco-cement was compared to other popular SCMs, namely coal fly ash and GGBF slag (NewCem). The following conclusions can be drawn:

- Eco-cement is likely a cementitious material due to its high C₂S content and its display of compressive strength gain when mixed with water.
- Eco-cement provides impressive early age strength, surpassing the compressive strength of straight OPC by 28% in 1-day strength measurements and greatly outperforming the

commercial benchmark SCMs used for comparison. This observation was complemented with findings from the Vicat needle tests measuring the time of setting, where Eco-cement shortened the setting time by 15% compared to the control OPC paste. This accelerator-like effect observed when using Eco-cement as an additive was likely due to the high amount of Cl^- containing minerals and salts in Eco-cement

- The ultimate strength of concrete was improved by 6% when partially replacing OPC binder by Eco-cement, reaching 51 MPa in 90 days of hydration.
- Higher replacement rates (50%) do not favor Eco-cement. Heat of hydration testing was used to determine that a higher amount of energy is released during the initial hydration stages of Eco-cement blended specimens. This likely led to a differential expansion between the Eco-cement and OPC, resulting in cracking and loss of strength.
- Eco-cement did not seem to influence the pore structure of OPC concrete. The absorption and volume of permeable pores remained relatively unchanged. The surface resistivity of OPC indicated that Eco-cement produces a more permeable pore structure. However, such a deduction could not be clearly drawn since Eco-cement seemed to alter the conductivity of the pore fluid due to the abundance of Cl^- ions in Eco-cement, thus rendering this test inconclusive.
- At 100 cycles of freeze/thaw testing, Eco-cement performed similarly (within 1%) to OPC and the commercial blends, indicating that Eco-cement does not negatively impact the frost resistance of concrete.

- Environmental leaching tests proved that the addition of Eco-cement to OPC still satisfied the requirements on heavy metals and chloride content according to the criteria set by Ontario Regulation 558 and U.S. EPA regulation.

Overall, Eco-cement proved to be an SCM that can partially replace OPC at 15% and drastically reduce the carbon footprint. All the while increasing the early age and ultimate strength of the concrete with no sacrifice to durability performance.

Future Works

In the future, other iterations of Eco-cement can be produced with an even higher MSWI residue percentage. Furthermore, by altering the blend design and the mineral composition, a better pozzolanic or cementitious material can be developed.

Although the high Cl^- of Eco-cement is hypothesized to lend an acceleration effect, it might have a negative impact on any steel reinforcement. The viability of using Eco-cement in steel reinforced concrete must be evaluated.

Further testing can be performed on Eco-cement to better evaluate its performance. Tests such as carbonation resistance, Mercury intrusion porosimetry (MIP), and rapid chloride penetration can help evaluate the durability of Eco-cement concrete. While tests such as Thermogravimetric Analysis (TGA) can provide more insight into composition of Eco-cement.

Finally, the environmental and economic benefits of Eco-cement can be quantified through a life cycle assessment. Furthermore, a study on the viability of converting a waste

incinerator into a local Eco-cement production plant can be performed. The benefits of using locally sourced materials and energy would greatly reduce the cost of Eco-cement production.

References

- A.GiesD, & Knöfel. (1986). Influence of alkalis on the composition of belite-rich cement clinkers and the technological properties of the resulting cements. *Cement and Concrete Research*, 411-422.
- A.Korpa, T.Kowald, & R.Trettin. (2008). Hydration behaviour, structure and morphology of hydration phases in advanced cement-based systems containing micro and nanoscale pozzolanic additives. *Cement and Concrete Research*, volume 38, 955-962.
- Ahmad, S. (2003). Reinforcement corrosion in concrete structures, its monitoring and service life prediction—a review. *Cement and Concrete Composites*, 459-471.
- AliNazari, & ShadiRiahi. (2010). The effect of TiO₂ nanoparticles on water permeability and thermal and mechanical properties of high strength self-compacting concrete. *Materials Science and Engineering: A*, 756-763.
- Ashraf, M. S., Ghouleh, Z., & Shao, Y. (2019). Production of eco-cement exclusively from municipal solid waste incineration residues. *Resources, Conservation and Recycling*, volume 149, 332-342.
- Beeghly, J. H. (2003). Recent experiences with lime - fly ash stabilization of pavement subgrade soils, base, and recycled asphalt. *International ash utilization symposium*. University of Kentucky.
- Bensted, J. (1987). Some applications of conduction calorimetry to cement hydration. *Advances in cement research*.
- Bouzoubaâ, N., & Fournier, B. (2003). Current Stituation of SCMs in Canada. *Materials Technology Laboratory Report*.
- Bullard, J. W., Jennings, H. M., Livingston, R. A., Nonat, A., Scherer, G. W., Schweitzer, J. S., . . . Thomas, J. J. (2011). Mechanisms of cement hydration. *Cement and Concrete Research*, 1208-1223.
- Cai, H., & Liu, X. (1998). Freeze-thaw durability of concrete: ice formation process in pores. *Cement and Concrete Research*, 1281-1287.
- Chen, X., & Shi, D. (2019). Influence of freeze–thaw cycles on apparent dynamic tensile strength, apparent dynamic fracture toughness and microstructure of concrete under impact loading. *European Journal of Environmental and Civil Engineering*.
- Chidiac, S., & Shafikhani, M. (2020). Electrical resistivity model for quantifying concrete chloride diffusion coefficient. *Cement and Concrete Composites*, Volume 113.
- Coppio, G. J., Lima, M. G., Lencioni, J. W., Cividanes, L. S., Dyer, P. P., & Silva, S. A. (2019). Surface electrical resistivity and compressive strength of concrete with the use of waste foundry sand as aggregate. *Construction and Building Materials*, 514 - 521.

- Dhawan, A., Gupta, N., Goyal, R., & Saxena, K. (2020). Evaluation of mechanical properties of concrete manufactured with fly ash, bagasse ash and banana fibre. *Materials Today: Proceedings*.
- Dhawana, A., Gupta, N., Goyal, R., & Saxenac, K. (2020). Evaluation of mechanical properties of concrete manufactured with fly ash, bagasse ash and banana fibre. *Materials Today: Proceedings*.
- Dhir, R., & McCarthy, M. (2006). *Concrete in the Service of Mankind: Appropriate concrete technology*. London: Taylor & Francis.
- Duan, P., Shui, Z., Chen, W., & Shen, C. (2013). Enhancing microstructure and durability of concrete from ground granulated blast furnace slag and metakaolin as cement replacement materials. *Journal of Materials Research and Technology*, Volume 2, 52-59.
- Duan, P., Shui, Z., Chen, W., & Shen, C. (2013). Enhancing microstructure and durability of concrete from ground granulated blast furnace slag and metakaolin as cement replacement materials. *Journal of Materials Research and Technology*, 52-59.
- Duran-Herrera, A., De-León-Esquivel, J., Bentz, D., & Valdez-Tamez, P. (2019). Self-compacting concretes using fly ash and fine limestone powder: Shrinkage and surface electrical resistivity of equivalent mortars. *Construction and Building Materials*, 50-62.
- E.Hekal, E., & A.Kishar, E. (1999). Effect of sodium salt of naphthalene-formaldehyde polycondensate on ettringite formation. *Cement and Concrete Research*, 1525-1540.
- El-Dieb, A. S., & Kanaan, D. M. (2018). Ceramic waste powder an alternative cement replacement – Characterization and evaluation. *Sustainable Materials and Technologies*, volume 17.
- Eriksson, O., Reich, M. C., Frostell, B., Björklund, A., Assefa, G., Sundqvist, J.-O., . . . Thyselius, L. (2005). Municipal solid waste management from a systems perspective. *Journal of Cleaner Production*, 31, 241-252.
- Erol, M., Küçükbayrak, S., & Ersoy-Meriçboyu, A. (2007). Production of glass-ceramics obtained from industrial wastes by means of controlled nucleation and crystallization. *Chemical Engineering Journal*, volume 132, 335-343.
- Ezema, I. C. (2019). Chapter 9 - Materials. *Sustainable Construction Technologies*, 237-262.
- Fantu, T., Alemayehu, G., Kebede, G., Abebe, Y., Selvaraj, S. K., & Paramasivam, V. (2021). Experimental investigation of compressive strength for fly ash on high strength concrete C-55 grade. *Materials Today: Proceeding*.
- Ghorbani, S., Taji, I., Brito, J. d., Negahban, M., Ghorbani, S., Tavakkolizadeh, M., & Ali, D. (2019). Mechanical and durability behaviour of concrete with granite waste dust as partial cement replacement under adverse exposure conditions. *Construction and Building Materials*, volume 194, 143-152.
- Ghorbani, S., Taji, I., Tavakkolizadeh, M., Davodi, A., & Brito, J. d. (2018). Improving corrosion resistance of steel rebars in concrete with marble and granite waste dust as partial cement replacement. *Construction and Building Materials*, volume 185, 110-119.

- Ghosh, S. N., Rao, P. B., Paul, A. K., & Raina, K. (1979). The chemistry of dicalcium silicate mineral. *Journal of Materials Science*, 1554–1566.
- Ghouleh, Z., & Shao, Y. (2018). Turning municipal solid waste incineration into a cleaner cement production. *Journal of Cleaner Production*, Volume 195, 268-279.
- Ghouleh, Z., Shao, Y., & Zhang, S. (2021). Performance of eco-concrete made from waste-derived eco-cement. *Journal of Cleaner Production*, 125758.
- Guo, X., Shi, H., Hu, W., & Wu, K. (2014). Durability and microstructure of CSA cement-based materials from MSWI fly ash. *Cement and Concrete Composites*, 26-31.
- Habert, G. (2014). 10 - Assessing the environmental impact of conventional and 'green' cement production. *Eco-efficient Construction and Building Materials*, 199-238.
- Hasegawa, M. (2014). Chapter 3.5 - Thermodynamic Basis for Phase Diagrams. *Treatise on Process Metallurgy*, 527-556.
- Hoornweg, D., & Bhada-Tata, P. (2012). What a waste: a global review of solid waste management. *Urban Dev Ser Knowl*, 15. 87-88.
- Hooton, R. (1987). Supplementary Cementing Materials. 247.
- Jalal, M., Fathi, M., & Farzad, M. (2013). Effects of fly ash and TiO₂ nanoparticles on rheological, mechanical, microstructural and thermal properties of high strength self compacting concrete. *Mechanics of Materials*, 11-27.
- Juenger, M., Provis, J., Elsen, J., Matthes, W., Hooton, D., Duchesne, J., . . . Belie, N. (2012). Supplementary Cementitious Materials for Concrete: Characterization Needs. *MRS Proceedings*.
- Katyal, N., Parkash, R., Ahluwalia, S., & Samuel, G. (1999). Influence of titania on the formation of tricalcium silicate. *Cement and Concrete Research*, 355-359.
- Khatrī, R., Sirivivatnanon, V., & Gross, W. (1995). Effect of different supplementary cementitious materials on mechanical properties of high performance concrete. *Cement and Concrete Research*, Volume 25, 209-220.
- Kikuchi, R. (2001). Recycling of municipal solid waste for cement production: pilot-scale test for transforming incineration ash of solid waste into cement clinker. *Resources, Conservation and Recycling*, Volume 31, 137-147.
- Kipkemboi, B., Zhao, T., Miyazawa, S., Sakai, E., Nito, N., & Hirao, H. (2020). Effect of C₃S content of clinker on properties of fly ash cement concrete. *Construction and Building Materials*, Volume 240.
- Kosajan, V., Wen, Z., Fei, F., Dinga, C. D., Wang, Z., & Zhan, J. (2020). The feasibility analysis of cement kiln as an MSW treatment infrastructure: From a life cycle environmental impact perspective. *Journal of Cleaner Production*, Volume 267.
- Lee, B. Y., & Kurtis, K. E. (2012). Proposed Acceleratory Effect of TiO₂ Nanoparticles on Belite Hydration: Preliminary Results. *Journal of the American Ceramics Society*, 365-368.

- Lin, K.-L., & Lin, C.-Y. (2012). Hydration Properties of Eco-Cement Pastes from. *Journal of the Air & Waste Management Association*, 2162-2906.
- Liu, X. C., Li, B. L., Qi, T., Liu, X. L., & Li, Y. J. (2013). Effect of TiO₂ on mineral formation and properties of alite-sulphoaluminate cement. *Materials Research Innovations*, 92-97.
- Lothenbach, B., Scrivener, K., & Hooton, R. (2011). Supplementary cementitious materials, . *Cement and Concrete Research*, Volume 41, 1244-1256.
- Makhloufi, Z., Bouziani, T., Hadjoudja, M., & Bederina, M. (2014). Durability of limestone mortars based on quaternary binders subjected to sulfuric acid using drying-immersion cycles. *Construction and Building Materials*, Volume 71, 579-588.
- Marthong, C., & Agrawal, T. (2012). Effect of Fly Ash Additive on Concrete Properties. *International Journal of Engineering Research and Applications*, Volume 2, 1986-1991.
- Mashaly, A. O., Shalaby, B. N., & Rashwan, M. A. (2018). Performance of mortar and concrete incorporating granite sludge as cement replacement. *Construction and Building Materials*, volume 169, 800-818.
- Massazza, F. (1993). Pozzolanic cements. *Cement and Concrete Composites*, Volume 15, Issue 4, 185-214.
- Mazouzi, W., Kacimi, L., Cyr, M., & Clastres, P. (2014). Properties of low temperature belite cements made from aluminosilicate wastes by hydrothermal method. *Cement and Concrete Composites*, 170-177.
- Meng Heng, K. M. (2004). Aging of concrete buildings and determining the pH value on the surface of concrete by using a handy semi-conductive pH meter. *Analytical Sciences, The Japan Society for Analytical Chemistry*, Vol 20.
- Mohseni, E., Naseri, F., Amjadi, R., Khotbehsara, M. M., & Ranjbar, M. M. (2016). Microstructure and durability properties of cement mortars containing nano-TiO₂ and rice husk ash. *Construction and Building Materials*, 656-664.
- Mor, S., Ravindra, K., Dahiya, R. P., & Chandra, A. (2006). Leachate Characterization and Assessment of Groundwater Pollution Near Municipal Solid Waste Landfill Site. *Environmental Monitoring and Assessment*, 434-456.
- Mu, R., Miao, C., Luo, X., & Sun, W. (2002). Interaction between loading, freeze-thaw cycles, and chloride salt attack of concrete with and without steel fiber reinforcement. *Cement and Concrete Research*, 1061-1066.
- Nayaka, R. R., Alengaram, U. J., Jumaat, M. Z., Yusoff, S. B., & Alnahhal, M. F. (2018). High volume cement replacement by environmental friendly industrial by-product palm oil clinker powder in cement – lime masonry mortar. *Journal of Cleaner Production*, volume 190, 272-284.
- Nazari, A., & Riahi, S. (2010). The effect of TiO₂ nanoparticles on water permeability and thermal and mechanical properties of high strength self-compacting concrete. *Materials Science and Engineering: A*, 756-763.

- Neuwald, A. D. (2010). Supplementary Cementitious Materials. *National Precast Concrete Association, Precast Magazines*.
- Ollivier, J., Maso, J., & B. Bourdette. (1995). Interfacial transition zone in concrete. *Advanced Cement Based Materials*, 30-38.
- Porras, Y., Jones, C., & Schmiedeke, N. (2020). Freezing and Thawing Durability of High Early Strength Portland Cement Concrete. *Journal of Materials in Civil Engineering*.
- Praveenkumar, T., Vijayalakshmi, M., & Meddah, M. (2019). Strengths and durability performances of blended cement concrete with TiO₂ nanoparticles and rice husk ash. *Construction and Building Materials*, 343-351.
- Praveenkumar, T., Vijayalakshmi, M., & Meddah, M. (2019). Strengths and durability performances of blended cement concrete with TiO₂ nanoparticles and rice husk ash. *Construction and Building Materials*, 343-351.
- Pruckner, F., & Gjrv, O. (2004). Effect of CaCl₂ and NaCl additions on concrete corrosivity. *Cement and Concrete Research*, 1209-1217.
- Quina, M. J., Bordado, J. C., & Quinta-Ferreira, R. M. (2007). Treatment and use of air pollution control residues from MSW incineration: An overview. *Waste Management*, 28, 2097-2121.
- Quina, M. J., Bordado, J. C., & Quinta-Ferreira, R. M. (2014). Recycling of air pollution control residues from municipal solid waste incineration into lightweight aggregates. *Waste Management*, volume 34, 430-438.
- Ramachandran, V. (1996). 5 - Accelerators. In V. Ramachandran, *Concrete Admixtures Handbook (Second Edition)* (pp. 185-285,). William Andrew Publishing.
- Rasanen, V., & Penttala, V. (2004). The pH measurement of concrete and smoothing mortar using a concrete powder suspension. *Cement and Concrete Research*, 813-820.
- Rashad, A. M. (2018). An overview on rheology, mechanical properties and durability of high-volume slag used as a cement replacement in paste, mortar and concrete. *Construction and Building Materials*, Volume 187, 89-117.
- Regourd, M., Thomassin, J., Baillif, P., & Touray, J. (1983). Blast-furnace slag hydration. Surface analysis. *Cement and Concrete Research*, 549-556.
- Reike, D., Vermeulen, W. J., & Witjes, S. (2018). The circular economy: New or Refurbished as CE 3.0? — Exploring Controversies in the Conceptualization of the Circular Economy through a Focus on History and Resource Value Retention Options. *Resources, Conservation and Recycling*, 135, 246-264.
- Richardson, A., Coventry, K., & Bacon, J. (2011). Freeze/thaw durability of concrete with recycled demolition aggregate compared to virgin aggregate concrete. *Journal of Cleaner Production*, 272-277.
- Richardson, I. G., & Groves, G. W. (1992). Microstructure and microanalysis of hardened cement pastes involving ground granulated blast-furnace slag. *Journal of Material Science*, 6204-6212.

- Richardson, I. G., Wilding, C. R., & Dickson. (1989). The hydration of blastfurnace slag cements. *Advances in Cement Research*, 147-157.
- Saint-Jean, S., Jøns, E., Lundgaard, N., & Hansen, S. (2005). Chlorellestadite in the preheater system of cement kilns as an indicator of HCl formation. *Cement and Concrete Research*, 431-437.
- Santos, R. M., Mertens, G., Salman, M., Cizer, Ö., & Gerven, T. V. (2013). Comparative study of ageing, heat treatment and accelerated carbonation for stabilization of municipal solid waste incineration bottom ash in view of reducing regulated heavy metal/metalloid leaching. *Journal of Environmental Management*, volume 128, 807-821.
- Sauvat, N., Sell, R., Mougél, E., & Zoulalian, A. (1999). A Study of Ordinary Portland Cement Hydration With Wood by Isothermal Calorimetry. *Laboratory of Chemical Processes*, 104-108.
- Schneider, M., Romer, M., Tschudin, M., & Bolio, H. (2011). Sustainable cement production – present and future. *Cement and Concrete Research*, 642-650.
- Schöler, A., Lothenbach, B., Winnefeld, F., Haha, M. B., Zajac, M., & Ludwig, H.-M. (2017). Early hydration of SCM-blended Portland cements: A pore solution and isothermal calorimetry study. *Cement and Concrete Research*, 71-82.
- Schutter, G. (1999). Hydration and temperature development of concrete made with blast-furnace slag cement. *Cement and Concrete Research*, 143-149.
- Schutter, G., & Taerwe, L. (1995). General hydration model for portland cement and blast furnace slag cement. *Cement and Concrete Research*, 593-604.
- Setina, J., Gabrene, A., & Juhnevica, I. (2013). Effect of Pozzolanic Additives on Structure and Chemical Durability of Concrete. *Procedia Engineering*, Volume 57, 1005-1012.
- Shaban, W. M., Elbaz, K., Yang, J., Thomas, B. S., Shen, X., Li, L., . . . Li, L. (2021). Effect of pozzolan slurries on recycled aggregate concrete: Mechanical and durability performance. *Construction and Building Materials*, Volume 276.
- Shang, D., Wang, M., Xia, Z., Hu, S., & Wang, F. (2017). Incorporation mechanism of titanium in Portland cement clinker and its effects on hydration properties. *Construction and Building Materials*, 344-349.
- Shang, H.-S., & Yi, T.-H. (2013). Freeze-Thaw Durability of Air-Entrained Concrete. *The Scientific World Journal*.
- Sharholi, M., Ahmad, K., Mahmood, G., & Trivedi, R. C. (2008). Municipal solid waste management in Indian cities—A review. *Waste management*, 459-467.
- Shen, F., Liu, J., Dong, Y., & ChenkaiGu. (2018). Insights into the effect of chlorine on arsenic release during MSW incineration: An on-line analysis and kinetic study. *Waste Management*, Volume 75, 327-332.
- Shetty, M. S. (2005). *Concrete Technology*. New Delhi: Chand & Company Ltd.

- Shia, C., & Qianb, J. (2000). High performance cementing materials from industrial slags — a review. *Resources, Conservation and Recycling*, Volume 29, 195-207.
- Shimoda, T., & Yokoyama, S. (1999). Eco-cement: a new Portland cement to solve municipal and industrial waste problems. *Proceedings of the International Conference Held at the University of Dundee*, (pp. 17-30).
- Singh, M., Kapur, P., & Pradip, A. (2008). Preparation of alinite based cement from incinerator ash. *Waste Management*, 1310-1316.
- Środek, D., Galuskina, I. O., Galuskin, E., Dulski, M., Książek, M., Kusz, J., & Gazeev, V. (2018). Chlorellestadite, $\text{Ca}_5(\text{SiO}_4)_1.5(\text{SO}_4)_1.5\text{Cl}$, a new ellestadite- group mineral from the Shadil-Khokh volcano, South Ossetia. *Mineralogy and Petrology*, 743–752.
- Środek, D., Galuskina, I., Galuskin, E., Dulski, M., Książek, M., Kusz, J., & Gazeev, V. (2018). Chlorellestadite, $\text{Ca}_5(\text{SiO}_4)_1.5(\text{SO}_4)_1.5\text{Cl}$, a new ellestadite- group mineral from the Shadil-Khokh volcano, South Ossetia. *Minerology and Petrology*, 743-752.
- Tang, J., Ylmén, R., Petranikova, M., Ekberg, C., & Steenari, B.-M. (2018). Comparative study of the application of traditional and novel extractants for the separation of metals from MSWI fly ash leachates. *Journal of Cleaner Production*, 143-154.
- Teoraneau, I., & Muntean, M. (1974). Proceedings of the 6th International Congress on the Chemistry of Cement. Stroiizdat, Moscow.
- Toan, V., Phalkong, P., Phuong, M., Buic, T., Ogawaa, Y., Kenji, & Kawaia. (2020). Effects of Shirasu natural pozzolan and limestone powder on the strength and aggressive chemical resistance of concrete. *Construction and Building Materials*, Volume 239.
- Wang, D.-h., Yao, X., Yang, T., Xiang, W.-r., Feng, Y.-t., & Chen, Y. (2021). Controlling the early-age hydration heat release of cement paste for deep-water oil well cementing: A new composite designing approach. *Construction and Building Materials*, Volume 285.
- Wang, P., Hu, Y., & Cheng, H. (2019). Municipal solid waste (MSW) incineration fly ash as an important source of heavy metal pollution in China. *Environmental Pollution*, Volume 252, 461-475.
- Wang, Y., Zhang, X., Liao, W., Wu, J., Yang, X., Shui, W., . . . Peng, H. (2018). Investigating impact of waste reuse on the sustainability of municipal solid waste (MSW) incineration industry using energy approach: A case study from Sichuan province, China. *Waste Management*, 252-267.
- Wu, K., Shi, H., & Guo, X. (2011). Utilization of municipal solid waste incineration fly ash for sulfoaluminate cement clinker production. *Waste Management*, 2001-2008.
- Yao, J., Kong, Q., Qiu, Z., Chen, L., & Shen, D. (2019). Patterns of heavy metal immobilization by MSW during the landfill process. *Chemical Engineering Journal*, Volume 375, .
- Yousuf, F., Wei, X., & Zhou, J. (2020). Monitoring the setting and hardening behaviour of cement paste by electrical resistivity measurement. *Construction and Building Materials*, Volume 252.

- Zareei, S. A., F. A., F. D., & M. A. (2017). Rice husk ash as a partial replacement of cement in high strength concrete containing micro silica: Evaluating durability and mechanical properties. *Case Studies in Construction Materials*, Volume 7, 73-81.
- Zhang, S., Ghoulleh, Z., & Shao, Y. (2020). Use of eco-admixture made from municipal solid waste incineration residues in concrete. *Cement and Concrete Composites*, volume 113.
- Zhao, H., Wu, X., Huang, Y., Zhang, P., Tian, Q., & Liu, J. (2021). Investigation of moisture transport in cement-based materials using low-field nuclear magnetic resonance imaging. *Magazine of Concrete Research*, 252-270.
- Zou, D., Qin, S., Liu, T., & Jivkov, A. (2021). Experimental and numerical study of the effects of solution concentration and temperature on concrete under external sulfate attack. *Cement and Concrete Research*, Volume 139.